Development of Non-toxic Quantum Dots for Flexible Display Applications

Research Report
of
Research Project funded by

'AOARD'

Period: August 09, 2011-August 08, 2013

PI: Prof. Kwang-Sup Lee
Nanophotonic Materials Laboratory
Department of Advanced Materials
Hannam University, Daejeon
Tel: +82-42-629-8857, Fax: +82-42-629-8854,
E-mail: kslee@hnu.kr / kslee8899@gmail.com

International Program Officer: Dr. Kenneth Caster
Asian Office of Aerospace Research & Development (AOARD), USA

Report Documentation Page

Form Approved
OMB No. 0704-0188

1. REPORT DATE	2. REPORT TYPE	3. DATES COVERED
14 NOV 2013	**Final**	**09-08-2011 to 08-08-2013**

4. TITLE AND SUBTITLE	5a. CONTRACT NUMBER
Development of Non-Toxic Quantum Dots for Flexible Display Applications	**FA23861114043**
	5b. GRANT NUMBER
	5c. PROGRAM ELEMENT NUMBER
6. AUTHOR(S) **Kwang-Sup Lee**	5d. PROJECT NUMBER
	5e. TASK NUMBER
	5f. WORK UNIT NUMBER
7. PERFORMING ORGANIZATION NAME(S) AND ADDRESS(ES) **Hannam University,461-6 Jeonmin-Dong, Yuseong-Gu,Daejeon 306-811,Korea (South),NA,NA**	8. PERFORMING ORGANIZATION REPORT NUMBER **N/A**
9. SPONSORING/MONITORING AGENCY NAME(S) AND ADDRESS(ES) **AOARD, UNIT 45002, APO, AP, 96338-5002**	10. SPONSOR/MONITOR'S ACRONYM(S) **AOARD**
	11. SPONSOR/MONITOR'S REPORT NUMBER(S) **AOARD-114043**

12. DISTRIBUTION/AVAILABILITY STATEMENT

Approved for public release; distribution unlimited

13. SUPPLEMENTARY NOTES

14. ABSTRACT

In order to achieve nanocrystals (NC) with stable and high photoluminescence (PL) and light harvesting efficiency (LHE), rare earth (RE) elements doped core/shell (CS) type semiconductors NC quantum dots (QDs) of group III-V elements were attempted with group II-VI element shell materials. An industrially adaptable low temperature ammine-ligands based process was chosen initially for the synthesis. Color control was achieved by tuning the size of the NCs. QDs having photoluminescence from infrared (IR) to blue were successfully synthesized. Quantum yield (QY) of these materials were attempted to increase by tuning the shell architecture. PL enhancement was observed with multiple shell growth indicating the inappropriate electronic (bandgap and band alignment) and surface (lattice mismatch) parameters for InP/ZnS binary CS system. A core/shell/shell (CSS) structure was attempted to overcome this lattice mismatch issue. Improvisation in efficiency was expected by converting them to upconverting nanoparticles (NPs). Doping with suitable IIB (Zn), VIIB (Mn) and RE elements (Ce, Er) can make them upconverting NPs free from environmental issue. Doping also could improve their thermal stability in display devices and increase the QY. Upconverting NPs are advantageous because in their hybrid photovoltaic devices they can produce high QY at IR region where solar spectrum has the highest photon flux density and also it is the region where most of the other materials fail. Doping these NCs with RE elements exhibited increase the optical efficiency. To improve the interparticle charge transport, surface modified versions of these nanoparticles were synthesized by replacing organic capping ligands on chemically synthesized nanocrystals with metal-free inorganic S2- and HS- ions which provided colloidal stability for the NCs in polar solvents.

15. SUBJECT TERMS **Quantum Dots, Flexible Electronics, Non-Toxic Materials; Photoluminescence, Core/Shell Nanostructures, Semiconductors, Light-Harvesting**					
16. SECURITY CLASSIFICATION OF:			17. LIMITATION OF ABSTRACT	18. NUMBER OF PAGES	19a. NAME OF RESPONSIBLE PERSON
a. REPORT **unclassified**	b. ABSTRACT **unclassified**	c. THIS PAGE **unclassified**	**Same as Report (SAR)**	**43**	

Standard Form 298 (Rev. 8-98)
Prescribed by ANSI Std Z39-18

1. Abstract

In order to achieve nanocrystals (NC) with stable and high photoluminescence (PL) and light harvesting efficiency (LHE), rare earth (RE) elements doped core/shell (CS) type semiconductors NC quantum dots (QDs) of group III-V elements were attempted with group II-VI element shell materials. An industrially adaptable low temperature ammine-ligands based process was chosen initially for the synthesis. Color control was achieved by tuning the size of the NCs. QDs having photoluminescence (PL) from infrared (IR) to blue were successfully synthesized. Quantum yield (QY) of these materials were attempted to increase by tuning the shell architecture. PL enhancement was observed with multiple shell growth indicating the inappropriate electronic (bandgap and band alignment) and surface (lattice mismatch) parameters for InP/ZnS binary CS system. A core/shell/shell (CSS) structure was attempted to overcome this lattice mismatch issue. Improvisation in efficiency was expected by converting them to upconverting nanoparticles (NPs). Doping with suitable IIB (Zn), VIIB (Mn) and RE elements (Ce, Er) can make them upconverting NPs free from environmental issue. Doping also could improve their thermal stability in display devices and increase the QY. Upconverting NPs are advantageous because in their hybrid photovoltaic devices they can produce high QY at IR region where solar spectrum has the highest photon flux density and also it is the region where most of the other materials fail. Doping these NCs with RE elements exhibited increase the optical efficiency. To improve the interparticle charge transport, surface modified versions of these nanoparticles were synthesized by replacing organic capping ligands on chemically synthesized nanocrystals with metal-free inorganic S^{2-} and HS^{-} ions which provided colloidal stability for the NCs in polar solvents.

2. Introduction

2-1. Background

In both organic and inorganic materials many physical phenomena are connected to their length scale between 1 and 100 nm. The knowledge that the control

of material properties can be achieved by tuning physical size of materials has widespread attention among science communities. In nm-scale structures, finite size effects give rise to novel electronic, magnetic, optical, and structural properties. The desire to identify, understand, and exploit the size-dependent properties of materials at the nanometer scale motivates the study of monodisperse nanometer-scale crystals, known as nanocrystals (NCs). Nanoparticles or nanoclusters of semiconductors materials are often called Quantum Dots (QDs). Nanocrystal QDs have efficient photoluminescent (PL) and electroluminescence (EL) properties, which make them suitable candidates for display applications. Usually QDs are consisted of an inorganic core with a size that comparable to Bohr exciton diameter of the corresponding bulk material, surrounded by an organic shell of ligands. Group II sulfides, selenides and tellurides formed by chemical synthesis are one of the most studied classes of light emitting materials with demonstrated potential in a wide range of applications.[1-6] CdSe QDs as the current workhorse have been demonstrated to possess a high capacity for such electroluminescence applications due to its broad color range.[7] However, CdSe is environmentally restricted and has little future in industry since Cd and Se are toxic elements.[8]

Semiconductors based on group III elements were found with a wide range of band gaps ranging from 6.2 eV, to 0.7 eV (Fig. 1). In terms of energy this spans from UV to IR region of the spectrum.[9-11] Group III elements are considered nontoxic since, they are used in *in vivo* experiments and clinical trials as medical imaging materials.[12-14] Of the various nano materials reported from this group, InP has been observed with efficient photoluminescence.[15-16] InP QDs have tunable PL properties as in the case of CdSe QDs.[8] Even though, other combinations such as InN, GaN, InGaN, InP/ZnS core shell structure, InGaAs/GaAs core-shell structure are also reported, reports of colloidal synthesis yielding good quality group III-V QDs with efficient PL properties are scarce.[17-19] Most of the nanocrystalline group III materials reported previously are typically large agglomerations with no reports of individual, colloidal solubility in organic solvents. Discrete colloidal nanoparticles with proper surface modification would enable large area deposition methods for building devices.

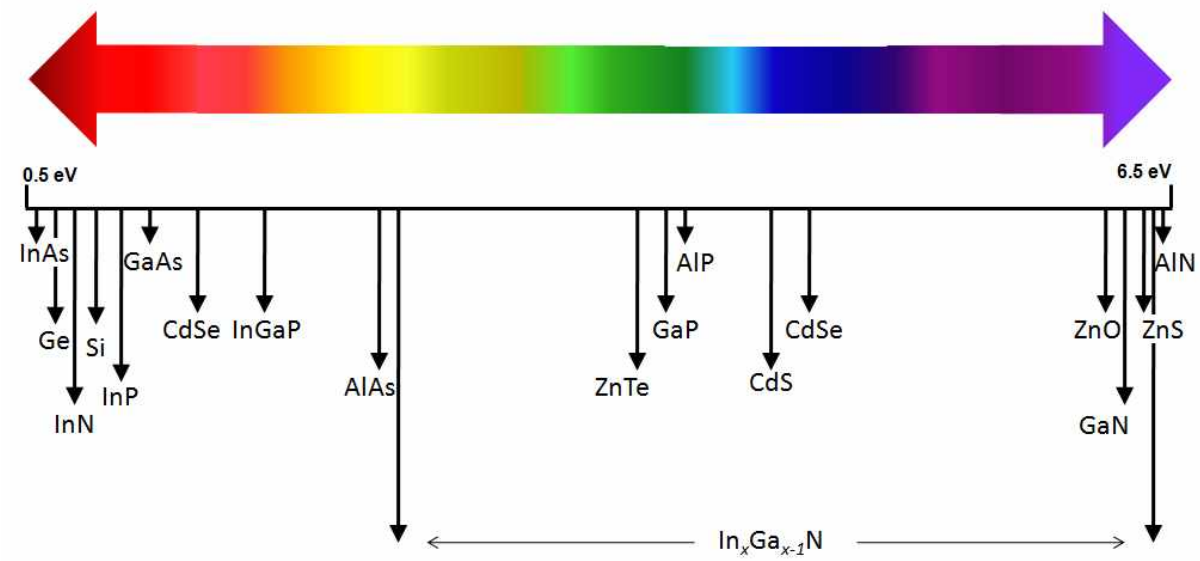

Fig. 1. Some important materials and their band gaps in bulk.[9-10,20-27]

2-2. Motivation

Compound semiconductors based on combinations of elements from Groups II and VI, III and V, III and VI, and IV and VI (Fig. 2) have significant impact on our day to day life. Materials such as CdSe, ZnS, CdS, CdTe, GaAs, aluminum gallium arsenide (AlGaAs), gallium nitride (GaN), indium phosphide (InP), zincselenide (ZnSe), cadmiumtelluride (CdTe), and copper indium gallium selenide $Cu(In_{1-x}Ga_x)Se_2$ (CIGS) have a wide variety of applications in satellite TV receivers, optical fiber communications, compact disk players, barcode readers, full color advertising displays, and solar cells. Group II is referred to the elements which belong to the group 12 of the current IUPAC convention. The elements of this group are Zn, Cd and Hg. Of these elements Zn and Cd are widely used in semiconductor preparation. Group III, presently known as group 13 according the IUPAC convention consists of the elements B, Al, Ga, In and Tl. The elements of importance as building block to semiconducting materials are Al, Ga and In. Group V and VI, presently know as group 15 and 16 composed of N, P, As, Sb, Bi and O, S, Se, Te, Po respectively. Though the thin films of these materials have been widely studies their quantum nanostructures like nanowire and QDs are expected to have greater applications.[28] Group II-VI semiconducting nanocrystals are

one of the most explored groups of materials. Wurtzite-structured cadmium selenide (CdSe) is an important II-VI semiconductor which has long been popular in the field of optoelectronics due to their quantum size-tunability of its properties leading to narrow emission wavelengths. Based on these properties they have been used as a model system for investigating a wide range of nanoscale electronic, optical, optoelectronic, and chemical processes. CdSe has a direct band gap of 1.8 eV. These quantum dots have been employed in laser diodes, nanosensing, and biomedical imaging.[29] However Cd being class A toxic element and Se being class B toxic element CdSe QDs are environmentally restricted and hence despite of their very interesting properties they have no preference in the industry.[8]

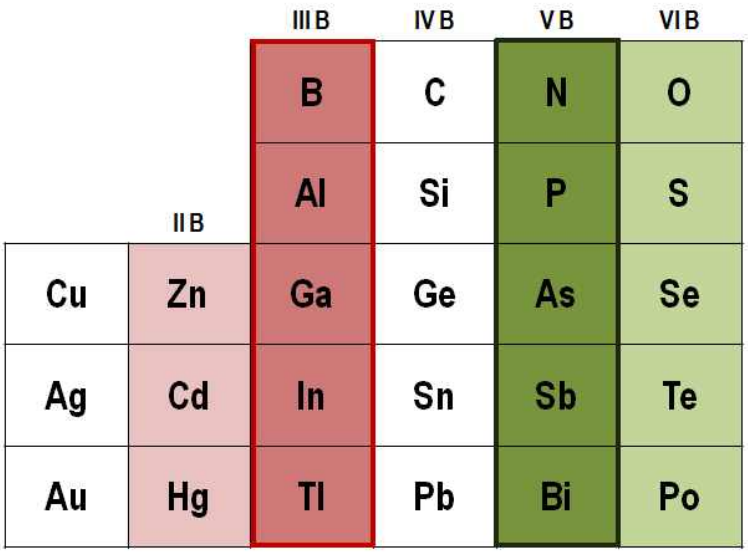

Fig. 2. Group II, III, IV, V and VI elements in periodic table.

III-V semiconductors could offer a broader emission color range similar to that of CdSe QDs but without intrinsic toxicity. Group III based material growth is subject to numerous challenges that have impeded the development and study of their compounds such as InP, GaP, GaN, InN, InGaP and InGaN. Epitaxial method is one of the most affordable methods for high quality crystal growth for many Group III based materials. Although some progress has been made in bulk GaN growth, lattice mismatch with the substrates induces the formation of defects and dislocations that

restrict film thickness and reduce device applicability. Another challenge arises is growth temperature. Even though, a few group III materials like, GaN has a high decomposition temperature that makes it amenable for fast growth by vapor-phase epitaxy (VPE), most other group III based materials suffer a much lower decomposition temperature. In the case of InN a temperature between 500-650 ^{o}C, that hinders defect free film growth. The extremely different growth conditions for GaN and InN suggests InGaN would be a difficult material to grow. This causes a miscibility gap preventing full band gap tunability between 0.7-3.4 eV. There have been no reports so far that produce a full compositional tunability in thin films.

Switching to the nano growth regime offers a new set of tools and conditions for synthesizing these materials. Moreover colloidal synthesis does not require a substrate. Unlike thin film growth processes, nanoparticle growth protocols, especially in solution processes such as solvothermal methods, can be conducted at lower temperatures (< 200 ^{o}C) and less extreme reaction environments, avoiding high pressure and toxic gases.[30] With regards specifically to InGaN, full compositional tunability has been claimed in nanowires, though mild compositional modulation was observed for 70-90% indium, and the success is attributed to low processing temperatures and strain-relaxed nanowire growth.[31] It is clear that the rules governing thin film growth do not directly apply in the nano regime. Moving from nanowires into the quantum dot regime is further advantageous. Size shrinking really matters for materials by increased influence of surface interactions, and also colloidal nanoparticles can be manipulated through chemistry to change solubility and interparticle forces. In addition, quantum dots demonstrate quantum confinement, which is a powerful and versatile way to control the electrical and optical properties of the material. Suitable surface functionalization leads to highly desirable properties like self assembly; and enables tailoring of nanoparticles for a variety of applications.[32-33] In summary, a colloidal nanocrystal system of group III elements may offer important advances in the PL device fabrication by utilizing their increased application flexibility. Synthesis of high quality III-V QDs, is a challenging process. Existing problems surrounding III-V QDs include poor emission efficiency, poor control of size distribution, poor size tunability, and/or poor stability. Moreover,

the synthetic protocols for III-V QDs are more complicated than that for II-VI nanocrystals.

In this background, based on our previous experience in extensive studies on PL properties of organic as well as inorganic materials including QDs and their applications in optoelectronics,[34-41] we have designed syntheses and modifications of III-V QDs in order to get high QY nanomaterials for industrial use. Initial attempts were dedicated to develop good quality nanomaterials using various possible and potential combinations of the III-V elements. Latter modification of these nanocrystals by growing different types of shells with materials having higher bandgap compared to that of the core and surface ligand modification to improve the electronic properties of the NCs and processability.

3. Experimental

3-1. Synthesis of core/shell nanocrystals of group III-V elements

3-1-1. GaN NC synthesis

A modified adaptation of reported procedure[42] was followed to prepare GaN nanoparticles. 1.0 g of $GaCl_3$ was combined with 0.9 g of $LiN(CH_3)_2$ in 100 mL anhydrous hexane under an inert atmosphere and allowed to mix overnight. Afterwards, the mixture was left undisturbed for several days, allowing the LiCl precipitate to settle to the bottom of the flask. Under nitrogen or argon atmosphere, 10 mL of the hexane supernatant, which held the precursor dimer $Ga_2[N(CH_3)_2]_6$, was put in a 50 mL three-neck, round bottom, borosilicate glass flask with a glass stir bar. 2 mL of trioctylamine and 0.25 g of hexadecylamine were added to the flask. The flask was then sealed with rubber septum and brought out into a laboratory hood with a prepared condenser topped with a bubbler. Due the difficulties in handling and hazardous nature, instead of the ammonia gas reported in the original literature nitrogen gas was delivered into the sealed flask through a syringe needle piercing one septum, created a higher pressure inside the flask, which allowed the central septum to be removed and the flask attached

to the condenser without allowing backflow of air into the flask. The gas flow remained steady for the duration of the synthesis. A thermocouple through the third septum monitored the reaction temperature while the stir bar maintained homogeneity of the solution. During the beginning of the temperature ramp to 300 ^{o}C over 4 hours, the solution changes from transparent liquid to an opaque, milky white gel. Simultaneously, the temperature of the mixture rises linearly to approximately 90 ^{o}C, after which the rise slows while the hexane was slowly boiled out of the system through the bubbler. Once all the hexane was evaporated, the solution temperature continued to rise to 300 ^{o}C. The heater was turned off after 20 hours at 300 ^{o}C, and the flow of nitrogen was continued until the solution reach to room temperature. The final product was found insoluble in organic solvents or water. Attempts to solubilize it in water by sonicating with octylamine, as reported by the original literature were also failed. A transition electron micrograph (TEM) coupled with electron dispersive X-ray spectroscopy (EDS) of the reaction samples prepared from a water suspension showed that no nanoparticles are formed.

3-1-2. InP/ZnS core/shell synthesis in one-pot protocol

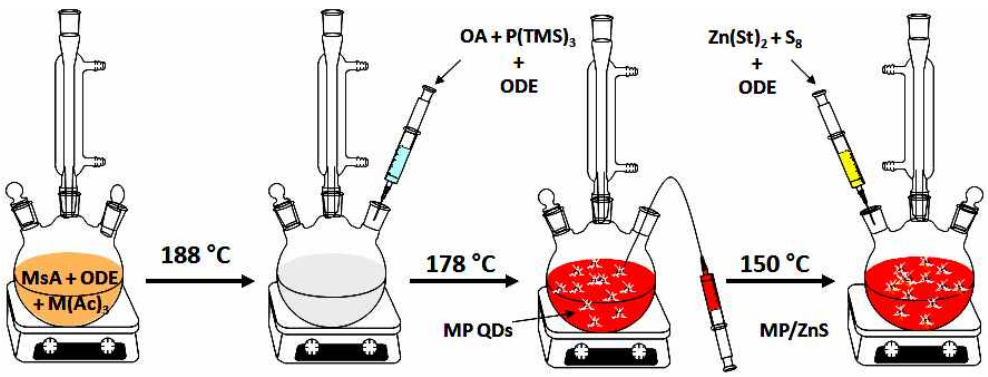

Fig. 3. Colloidal synthesis of group III phosphide QDs and group III phosphide/zinc sulfide core shell QDs in one pot protocol. Reagent abbreviations used, MsA: myristic acid, ODE: octadecene, $M(Ac)_3$: group III acetate, OA: octylamine, $P(TMS)_3$: tris(trimethylsilyl)-phosphine, MP QDs: group III phosphide quantum dots, $Zn(St)_2$: zinc stearate, S_8: sulfur, MP/ZnS: group III phosphide/ZnS core shell structure.

Method-1

The preparation of injection solution: 0.4 mmol of tris(dimethylamino)-phosphine ($P(NMe_2)_3$) and 4.8 mmol of 1-octylamine were dissolved in 3.0 mL 1-octadecene (ODE) in a glove box for injection. Then a 0.8 mmol of indium acetate ($In(OAc)_3$) and 2.9, 3.0 or 3.3 mmol of myristic acid (MA) in 5mL ODE were loaded into a three-neck flask. The mixture was heated to 188 ºC under nitrogen for 5 min. To this clear hot solution, $P(NMe_2)_3$/amine solution made in glove box was injected. The cold injection solution brought the reaction temperature down to 178 ºC for the growth of InP nanocrystals. To monitor the growth of the nanocrystals, aliquots were taken at different reaction times for absorption measurement.

For the growth of ZnS shell, the reaction solution was cooled down to 150 ºC. Typical synthesis of InP/ZnS core/shell nanocrystals was performed by thermal cycling. Zinc stearate (0.1 M in ODE) and sulfur (0.1 M in ODE) precursors (1.2 ml each) were added consequently to the reaction flask with the InP nanocrystals, waiting for 10 min between each injection at 150 ºC. After that, the temperature was increased to 220 ºC for 30 min to allow the growth of ZnS shell. Then the reaction temperature was cooled down to 150 ºC for further growth of core/shell nanocrystals by repeating the procedure but with a different amount of the precursor solutions (1.6 ml of zinc and sulfur precursors). When the synthesis was completely, the reaction was cooled down to room temperature. For purification, 10 mL of hexane was added to reaction solution, the unreacted compounds and byproducts were removed by successive methanol extraction until the methanol phase was clear. As prepared InP/ZnS nanocrystals were dispersed in chloroform.

Method-2

The preparation of injection solution: 0.4 mmol of tris(trimethylsilyl)phosphine ($P(TMS)_3$) and 4.8 mmol of 1-octylamine were dissolved in 3,0 mL 1-octadecene (ODE) in a glove box for injection. Then a 0.8 mmol of indium acetate ($In(OAc)_3$) and 2.9, 3.0 or 3.3 mmol of myristic acid (MA) in 5mL of ODE were loaded into a three-neck flask. The mixture was heated to 188 ºC under nitrogen for 5 min. To this clear hot solution $P(TMS)_3$/amine solution made in glove box was injected. The cold injection

solution brought the reaction temperature down to 178 ºC for the growth of InP nanocrystals. To monitor the growth of the nanocrystals, aliquots were taken at different reaction times for absorption measurement.

For the growth of ZnS shell, the reaction solution was cooled down to 150 ºC. Typical synthesis of InP/ZnS core/shell nanocrystals was performed by thermal cycling. Zinc stearate (0.1 M in ODE) and sulfur (0.1 M in ODE) precursors (1.2 ml each) were added consequently to the reaction flask with the InP nanocrystals, waiting for 10 min between each injection at 150 ºC. After that, the temperature was increased to 220 ºC for 30 min to allow the growth of ZnS shell. Then the reaction temperature was cooled down to 150 ºC for further growth of core/shell nanocrystals by repeating the procedure but with a different amount of the precursor solutions (1.6 ml zinc and sulfur precursors). When the synthesis was completely, the reaction was cooled down to room temperature. For purification, 10 mL of hexane was added to reaction solution, the unreacted compounds and byproducts were removed by successive methanol extraction until the methanol phase was clear. As prepared InP/ZnS nanocrystals were dispersed in chloroform.

Method-3

The preparation of injection solution: 0.4 mmol of tris(trimethylsilyl)phosphine ($P(TMS)_3$) and 4.8 mmol of 1-hexadecylamine were dissolved in 1-octadecene (ODE, 3.0 mL) in a glove box for injection. Then a 0.8 mmol of indium acetate ($In(OAc)_3$) and 2.9, 3.0 or 3.3 mmol of myristic acid (MA) in 5mL of ODE were loaded into a three-neck flask. The mixture was heated to 188 ºC under nitrogen for 5 min. To this clear hot solution $P(TMS)_3$/amine solution made in glove box was injected. The cold injection solution brought the reaction temperature down to 178 ºC for the growth of InP nanocrystals. To monitor the growth of the nanocrystals, aliquots were taken at different reaction times for absorption measurement.

For the growth of ZnS shell, the reaction solution was cooled down to 150 ºC. Typical synthesis of InP/ZnS core/shell nanocrystals was performed by thermal cycling. Zinc stearate (0.1 M in ODE) and sulfur (0.1 M in ODE) precursors (1.2 ml each) were added consequently to the reaction flask with the InP nanocrystals, waiting for 10 min

between each injection at 150 ºC. After that, the temperature was increased to 220 ºC for 30 min to allow the growth of ZnS shell. Then the reaction temperature was cooled down to 150 ºC for further growth of core/shell nanocrystals by repeating the procedure but with a different amount of the precursor solutions (1.6 ml zinc and sulfur precursors). When the synthesis was completely, the reaction was cooled down to room temperature. For purification, 10 mL of hexane was added to reaction solution, the unreacted compounds and byproducts were removed by successive methanol extraction until the methanol phase was clear. As prepared InP/ZnS nanocrystals were dispersed in chloroform.

3-1-3. Synthesis of core/shell/shell (CSS) type InP/ZnSe/ZnS NCs in one-pot protocol

Method-4

InP core was synthesized following the InP synthetic procedure reported before in Method-2. For the growth of ZnSe shell, the reaction solution was cooled down to 150 ºC. A 0.1 M of zinc stearate solution and 0.1 M of Se in trioctylphosphine (TOP) solution (1.2 mL each) were added consequently to the reaction flask with the InP nanocrystals, waiting for 10 min between each injection at 150 ºC. After that, the temperature was increased to 220 ºC for 30 min to allow the growth of ZnSe shell. The reaction mixture was again cooled down to 150 ºC for the growth of ZnS shell. Zinc stearate (0.1 M in ODE) and sulfur (0.1 M in ODE) precursors (1.2 ml each) were added consequently to the reaction flask with the InP/ZnSe nanocrystals, waiting for 10 min between each injection at 150 ºC. After that, the temperature was increased to 220 ºC for 30 min to allow the growth of ZnS shell.

Method-5

A stock solution of Se was made by degassing Se (0.744 g, 9.4 mmol) in 80 g of ODE at 100 °C for 20 min and subsequently heating the mixture under nitrogen at 200 °C for 2 h. During this time, the ODE/Se mixture changed from colorless to

orange-red and finally to yellow. The resulting transparent yellow solution was then cooled to room temperature where it remained stable for weeks under nitrogen.

InP core was synthesized following the procedure reported in Method-2. For the growth of ZnSe shell, the reaction solution was cooled down to 150 ºC. A 0.1 M of zinc stearate solution and 0.1 M of Se solution (stock solution previously prepared) (1.2 mL each) were added consequently to the reaction flask with the InP nanocrystals, waiting for 10 min between each injection at 150 ºC. After that, the temperature was increased to 220 ºC for 30 min to allow the growth of ZnSe shell. After this the reaction solution was again cooled down to 150 ºC for the growth of ZnS shell. Zinc stearate (0.1 M in ODE) and sulfur (0.1 M in ODE) precursors (1.2 ml each) were added consequently to the reaction flask with the InP/ZnSe nanocrystals, waiting for 10 min between each injection at 150 ºC. After that, the temperature was increased to 220 ºC for 30 min to allow the growth of ZnS shell.

3-1-4. Surface passivation of InP/ZnS core/shell NCs with simple inorganic metal-free ligands

Colloidal dispersions of different NCs with organic ligands were prepared in toluene and a solution of inorganic ligand was prepared in formamide (FA). For a typical ligand exchange using S^{2-} ions, 1mL of InP/ZnS NC solution (~2 mg/mL) was mixed with 1 mL of K_2S solution (5 mg/mL). The mixture was stirred for about 10 min leading to a complete phase transfer of InP/ZnS NCs from toluene to the FA phase. The phase transfer can be easily monitored by the color change of toluene (red to colorless) and FA (colorless to red) phases. The FA phase was separated out followed by triple washing with toluene to remove any remaining nonpolar organic species. The washed FA phase was then filtered through a 0.2 μm PTFE filter and ~1 mL of acetonitrile was added to precipitate out the NCs. The precipitate was redispersed in FA and used for further studies. Ligand exchange with HS^- was carried out in a similar manner. The solutions of S^{2-} capped NCs when handled in inert atmosphere the colloidal stability was found for months, while when handled in air their colloidal stability preserved only for several days.

3-1-5. Synthesis of Ce^{3+} ions doped InP/ZnS core/shell NCs in one-pot protocol

InP core was synthesized following the InP synthetic procedure reported before in Method-2. After the desired growth time, the reaction mixture was cooled to 130 ^{o}C. A not well dissolved cerium acetate ($Ce(OAc)_3$) slurry in ODE was made by heating 5 and 10 mol % $Ce(OAc)_3$ in 2 mL ODE at 200 ^{o}C. This slurry was added to the reaction mixture at 130 ^{o}C in one-shot. The reaction mixture was further heated to 210 ^{o}C for the diffusion of Ce^{3+} ions into the InP nanocrystals. For the growth of ZnS shell, the reaction solution was cooled down to 150 ºC. Zinc stearate (0.1 M in ODE) and sulfur (0.1 M in ODE) precursors (1.2 ml each) were added consequently to the reaction flask with the InP/ZnSe nanocrystals, waiting for 10 min between each injection at 150 ºC. After that, the temperature was increased to 220 ºC for 30 min to allow the growth of ZnS shell.

3-1-6. In(Zn)P/ZnS core/shell synthesis

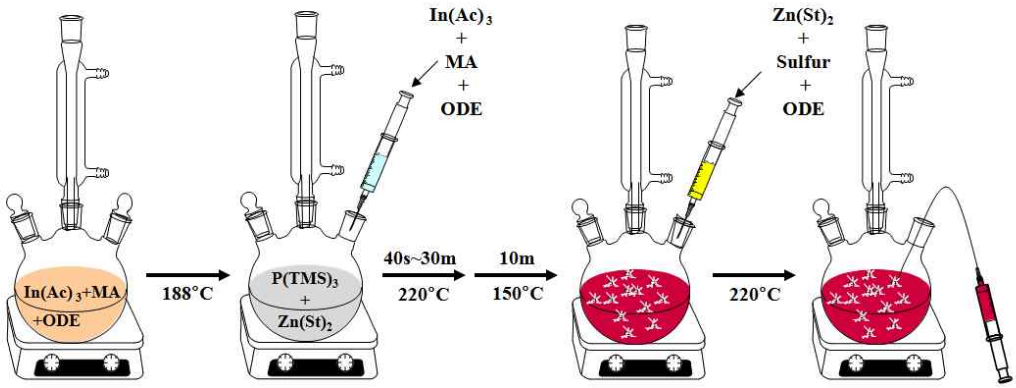

Fig. 4. Scheme for colloidal synthesis of group III (Zinc) phosphide QDs and group III (Zinc) phosphide/zinc sulfide core shell QDs in one pot protocol (*Method-1*). Reagent abbreviations used, MA: myristic acid, ODE: octadecene, $In(Ac)_3$: group III acetate, $P(TMS)_3$: tris(trimethylsilyl)phosphine, $Zn(St)_2$: zinc stearate, S_8: sulfur.

Method-6

The preparation of injection solution: 0.8 mmol of indium acetate ($In(OAc)_3$) and 2.9, 3.0 or 3.3 mmol of myristic acid (MA) were dissolved in 10mL of ODE in a glove box and heated it up to 188 ºC for 20 min. Under the N_2 atmosphere the mixture of 0.8 mmol of tris(trimethylsilyl)phosphine ($P(TMS)_3$) and 0.8 mmol of zinc stearate is mixed. In this mixture the heated former solution is injected as shown in the above Figure 4. The flask was then sealed with rubber septum and brought out into a laboratory hood with a prepared condenser topped with a bubbler. And then the solution is heated up to 220 ºC. To prepare the QDs with different optical energies the growth time of NC (nanocrystals) is controlled. For the growth of ZnS shell, typical synthesis of In(Zn)P/ZnS core/shell nanocrystals was performed by thermal cycling. The reaction solution was cooled down to 150 ºC. To this clear hot solution 3 ml of zinc stearate (0.8 mmol) and sulfur (0.8 mmol) in ODE (5 ml) precursors were taken in syringe and then added. The whole mixture is heated to 220 ºC for 30 min. When the synthesis is completed, the reaction mixture was cooled down to room temperature. For purification, 10 mL of chloroform was added to reaction solution, the unreacted compounds and byproducts were removed by successive acetone extraction until the acetone phase was clear. As prepared In(Zn)P/ZnS nanocrystals were dispersed in chloroform.

Method-7

For the preparation of QD core the previous *Method 6* is employed except the 3.3 mmol of myristic acid (MA) used. For the growth of ZnS shell, typical synthesis of In(Zn)P/ZnS core/shell nanocrystals was performed by thermal cycling. The reaction solution is cooled down to 150 ºC. To this clear hot solution only 3 ml of sulfur (0.8 mmol) in ODE (5 ml) precursors is taken with syringe and then added. And the whole mixture is heated to 220 ºC for 30 min.

Method-8

The preparation of injection solution: 0.8 mmol of indium acetate ($In(OAc)_3$) and 2.9, 3.0 or 3.3 mmol of myristic acid (MA) were dissolved in 10mL of ODE in a glove box and heated it up to 188 ºC for 20 min. A 0.8 mmol solution of tris(trimethylsilyl)-

phosphine ($P(TMS)_3$) and 0.8 mmol zinc stearate are mixed in N_2 atmosphere. In this mixture the heated injection solution is added. The flask was then sealed with a rubber septum and brought out into a laboratory hood with a prepared condenser topped with a bubbler; and heated up to 220 ºC. To prepare the QDs with different optical energies the growth time of NC (nanocrystals) is controlled. For the growth of ZnS shell, typical synthesis of In(Zn)P/ZnS core/shell nanocrystals was performed by thermal cycling. The reaction solution was cooled down to 150 ºC. To this clear hot solution 3 ml of Zinc stearate (0.8 mmol) and sulfur (0.8 mmol) precursors in ODE (5 ml) is added using a syringe. The whole mixture is heated to 220 ºC for 30 min. We prepared core/shell QDs with different ZnS shell thickness by above thermal cycling 1-8 times.

3-1-7. Synthesis of Mn^{3+} ions doped In(Zn)P/ZnS core/shell NCs in one-pot protocol

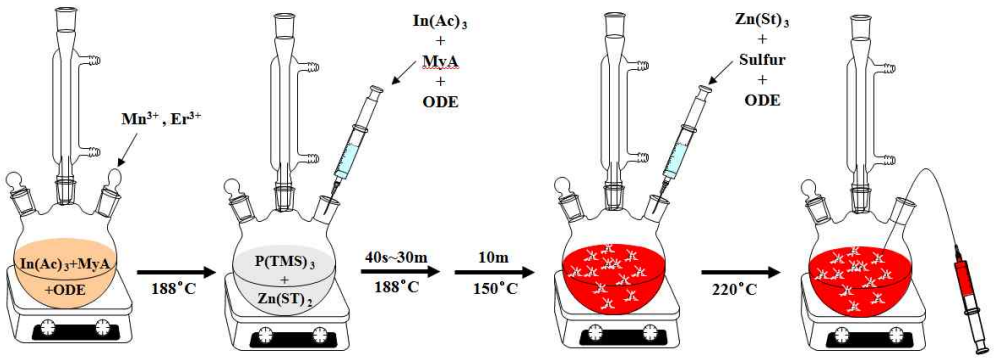

Fig. 5. Scheme of colloidal synthesis for group III (Zinc) phosphide QDs doped with *Mn^{3+} ions* and group III (Zinc) phosfide/zinc sulfide core shell QDs in one pot process. Reagent abbreviations used, MA: myristic acid, ODE: octadecene, $In(Ac)_3$: group III acetate, $P(TMS)_3$: tris(trimethylsilyl)phosphine, $Zn(St)_2$: zinc stearate, S_8: sulfur.

In(Zn)P QD cores doped with with Mn^{3+} ions in different concentration of 5 % and 10 % are synthesized as the same route as the In(Zn)P synthetic procedure described in *Method-6*. In the glove box the injection solution of indium acetate ($In(OAc)_3$) 0.8 mmol, myristic acid (MA) 3.3 mmol and 5 mol % (or 10 mol %) of manganese acetate ($Mn(OAc)_3$) is prepared in 10mL of ODE in a 100 mL three-neck flask and heated for 20 min at 188 ºC. Under the N_2 atmosphere 0.8 mmol of

tris(trimethylsilyl)phosphine ($P(TMS)_3$) and 0.8 mmol of zinc stearate is mixed. In this mixture the heated former solution is injected as shown in the above Figure 5. The flask was then sealed with rubber septum and brought out into a laboratory hood with a prepared condenser topped with a bubbler. The solution is heated up to 220 ºC. To prepare the QDs with different emission properties the growth time of nanocrystals is controlled. For the growth of ZnS shell, typical synthesis of In(Zn)P/ZnS core/shell nanocrystals was performed by thermal cycling. The reaction solution was cooled down to 150 ºC. To this clear hot solution 3 ml of zinc stearate (0.8 mmol) and sulfur (0.8 mmol) in ODE (5 ml) precursors is taken with syringe and then added. And the whole mixture is heated to 220 ºC for 30 min. When the synthesis was complete, the reaction was cooled down to room temperature. For purification, 10 mL of chloroform was added to reaction solution, the unreacted compounds and byproducts were removed by successive acetone extraction until the acetone phase was clear. As prepared In(Zn)P/ZnS nanocrystals were dispersed in chloroform.

3-1-8. Synthesis of Er^{3+} ions doped In(Zn)P/ZnS core/shell NCs in one-pot protocol

In(Zn)P QD cores doped with with Er^{3+} ions in different concentration of 5 % and 10 % are synthesized as the same route as the In(Zn)P synthetic procedure described in *Method-6*. In the glove box, the injection solution of indium acetate ($In(OAc)_3$) 0.8 mmol, myristic acid (MA) 3.3 mmol and 5 mol % (or 10 mol %) of erbium acetate ($Er(OAc)_3$) is prepared in 10mL of ODE in a 100 mL three-neck flask and heated for 20 min at 188 ºC. Under the N_2 atmosphere 0.8 mmol of tris(trimethylsilyl)phosphine ($P(TMS)_3$) and 0.8 mmol of zinc stearate is mixed. In this mixture the heated former solution is injected as shown in the above Figure 5. The shelling process is the same as described in *Mehtod 8*. Work-up and separation is followed as the previous procedures.

4. Results and Discussions

4-1. Synthesis of nanocrystals of group III-V elements

Colloidal semiconductor nanocrystals (NCs), also termed ‘‘quantum dots’’ (QDs), are composed of an inorganic core, made up of a few hundred to a few thousand atoms, surrounded by an organic outer layer of surfactant molecules (ligands). Their small size results in an observable quantum confinement effect, defined by an increasing bandgap accompanied by the quantization of the energy levels to discrete values. This effect is accompanied by an exaltation of the coulomb interaction between the charge carriers.

The tunable optical and electronic properties of quantum dots make them ideal building blocks in nanoscale photonic, photovoltaic, and light-emitting diode (LED) device applications. The most widely utilized quantum dots to date are II–VI semiconductor nanocrystals such as cadmium selenide, cadmium sulfide, and cadmium telluride. Presence of poisonous heavy metals makes these nanostructures unattractive for large scale uses such as that in industry. III-V QDs are very powerful alternative to II-VI QDs which are under intensive investigation in the recent years. An III-V material GaN was attempted to synthesize for photoluminescence application. A modified adaptation of a reported procedure[42] was followed to synthesize GaN nanoparticles. Instead of ammonia gas used in the reported procedure nitrogen gas was used during the synthesis due to the hazardous nature and difficulties in handling of ammonia (see ‘Experimental’ 3-1-1). $GaCl_3$ was combined with $LiN(Me)_2$ in hexane at inert conditions and kept stirring for several days. This mixture was treated with trioctylamine and hexadecylamine. Nitrogen was bubbled through the reactor instead of ammonia. Reaction mixture was heated to 300 ^oC over a period of 4 h. After extraction of the material it was found that the reaction failed to produce required GaN nanocrystals. Experiments with different combinations of temperature, time and reactants were attempted to solve the issue. The replaced ammonia gas with N_2 may be the reason which made the reaction difficult to produce GaN nanocrystals. Due to the safety reasons and difficulties in handling ammonia gas in the laboratory conditions, a

potential alternative and less frequently reported InP/ZnS core/shell (CS) NCs has been attempted instead of GaN. CS structures are very important when the quantum yield and stability of these sensitive materials are considered. In NCs, the nanometric crystal size of the core results in a very high surface to volume ratio. In the naked core alone structures, the co-ordination sphere of this surface atoms partially occurs via complex formation with the stabilizing ligands. Nevertheless, a significant fraction of these organically passivated core NCs typically exhibit surface related trap states acting as fast non-radiative de-excitation channels for photogenerated charge carriers, thereby reducing the fluorescence quantum yield (QY). Shell overgrowth with a second semiconductor to form CS systems is an important strategy to improve NCs' surface passivation.

When the bandgap of the shell material is larger than that of the core, both electrons and holes are confined in the core and such type of CS systems are classified as type-I. In such CS NCs, the shell is used to passivate the surface of the core in order to improve its optical properties. Bulk bandgap of ZnS is higher than that of InP. Hence InP/ZnS system act as a type-I quantum dot. Apart from electron confinement, ZnS shell physically separates the surface of the optically active core from its surrounding medium. Consequently, the sensitivity of the NC towards the local environment like oxygen or water molecule is reduced. With respect to core NCs, CS systems exhibit generally enhanced stability against photodegradation. At the same time, shell growth reduces the number of surface dangling bonds, which can act as trap states for charge carriers and thereby reduce the fluorescence QY. At the same time it significantly improves the fluorescence QY and stability against photobleaching, the shell growth is accompanied by a small red shift of the excitonic peak in the UV/Vis absorption spectrum and the photoluminescence (PL) wavelength. This observation is attributed to a partial leakage of the exciton into the shell material. A one pot protocol was tailored to synthesize InP/ZnS CS structures.

An ammine based reaction was chosen to design an industrially preferred low temperature protocol. A modified version of a reported procedure[8] was adapted for the initial attempts (see 'Experimental' 3-1-2, Method-1). Indium myristate was prepared *in situ* by treating indium acetate and myristic acid in ODE at 188 ^{o}C. $P(NMe_2)_3$ was used

as the phosphorous donor. The reaction with different combinations of reaction time, reactant amounts and temperatures below 200 ^{o}C produced InP NCs. The reaction mixture was cooled to 150 ^{o}C and a 0.1 M solution of Zn and S precursors (both 1.2 mL each) were added to grow a single layer of shell. For the shell growth the reaction temperature was raised to 220 ^{o}C over a period of 30 minutes. All the samples resulted with PL emission only in blue region. It may be due to the difficulty in stabilizing the free phosphide in the reaction conditions prevents growth of NCs to a larger size. Attempts with different alkylamines like decyl amine (DA) and dodecyl amine (DDA) are in progress to solve this issue.

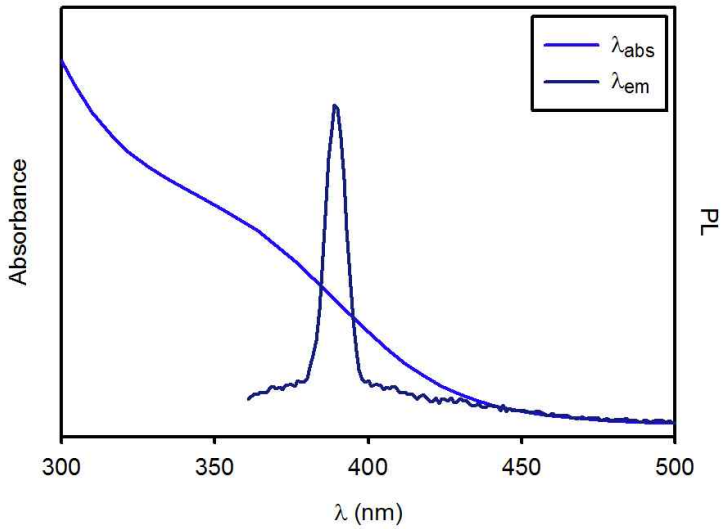

Fig. 6. UV-vis and PL spectra of InP/ZnS core shell QDs prepared from indium acetate (4 mmol) and tris(dimethylamino)phosphine (8mmol) at 178 ^{o}C.

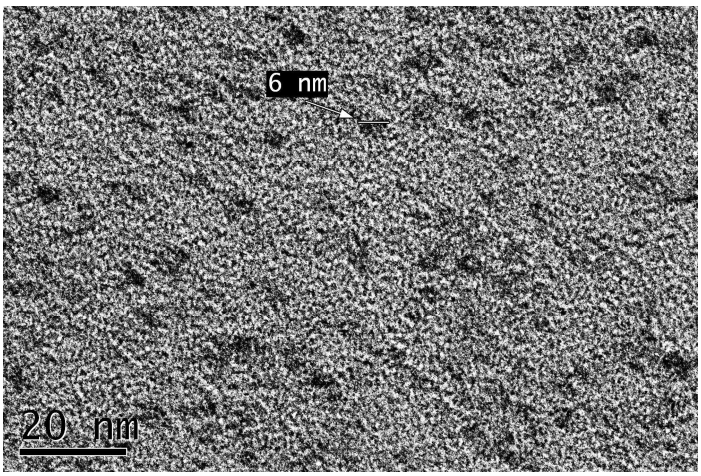

Fig. 7. TEM image of InP/ZnS core/shell red emitting QDs prepared from indium acetate (4 mmol) and tris(trimethylsilyl)phosphine (8mmol) at 178 ^{o}C.

A one-pot CS nanoparticle synthesis with tris(trimethylsilyl)phosphine ($P(TMS)_3$) as phosphorous donor was attempted and it was successful in producing NCs with PL ranging from infrared (IR) to blue region. This reaction typically followed the previously described protocol.

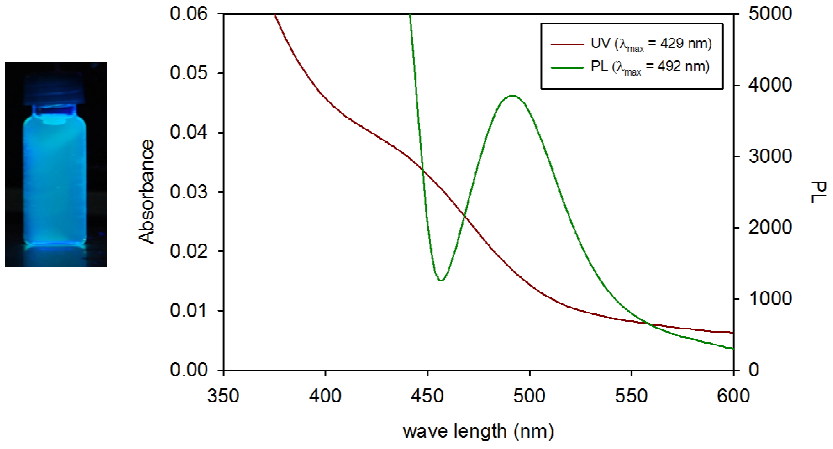

Fig. 8. Photo taken under the 365 nm UV radiation(Left) and UV-vis and PL spectra (Right) of InP/ZnS core shell blue QDs prepared from indium acetate (4 mmol) and tris(trimethylsilyl)phosphine (8mmol) at 178 ^{o}C.

Time of reaction was chosen as the variable to tune the color of PL by varying the size of the NCs. Varying amounts of myristic acid (MyA) used in the one-pot protocol also plays an important role in determining the size and their uniform distribution. For larger size NCs at elevated temperatures, excess amounts of MyA in the medium will support the stability of indium myristate and hence a slow and continuous supply of In^{3+} is ensured for long reaction time. While a relatively lesser amount of MyA ensures immediate consumption of In^{3+} ensuring the small NCs with relatively uniform distribution.

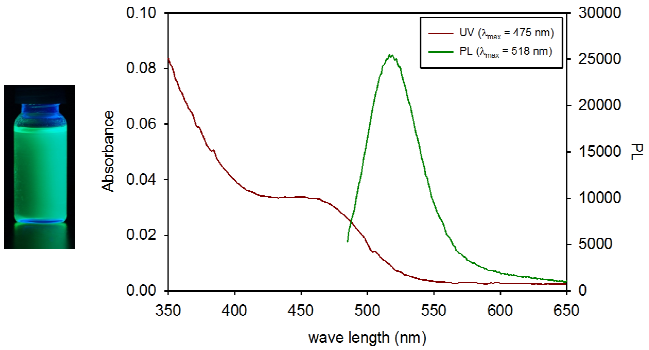

Fig. 9. UV-vis and PL spectra of InP/ZnS core shell green emitting QDs prepared from indium acetate (4 mmol) and tris(trimethylsilyl)phosphine (8mmol) at 178 ^{o}C.

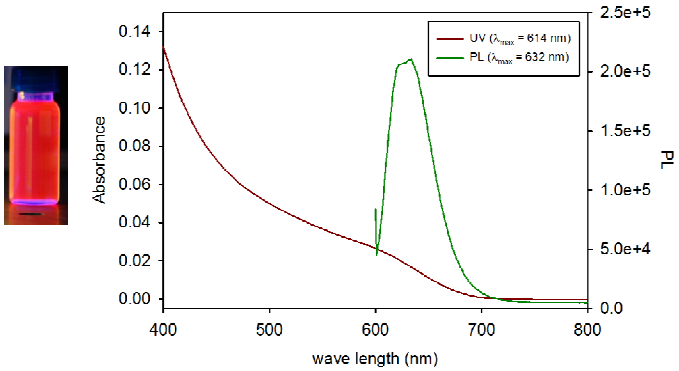

Fig. 10. Photo taken under the 365 nm UV radiation (Left) and UV-vis and PL spectra (Right) of InP/ZnS core shell red QDs prepared from indium acetate (4 mmol) and tris(trimethylsilyl)phosphine (8mmol) at 178 ^{o}C.

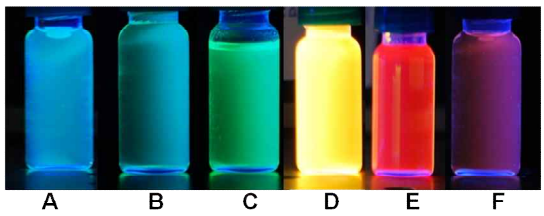

Fig. 11. Photo taken under the 365 nm UV radiation with different color emitting InP/ZnS QDs prepared from indium acetate (4 mmol) and tris(trimethylsilyl)phosphine (8mmol) at 178 ^{o}C; (**A**) λ_{em} = 492 nm, (**B**) 505 nm, (**C**) 526 nm, (**D**) 604 nm, (**E**) 632 nm, (**F**) 809 nm.

While a 20 seconds reaction produced blue color QDs, a 5 minutes reaction produced green dots and a one hour reaction produced red dots. A relatively broader (50 nm) full width at half maximum (FWHM) for PL were observed for NCs obtained through this method. These materials are generally reported with broader FWHM.

4-2. Optical Properties of Nanocrystals of Group III-V Elements containing Zn; In(Zn)P

The Optical characteristics of In(Zn)P/ZnS core/shell (CS) NCs (***3-1-6.*** *Method-1*) has been evaluated by their UV-vis absorption and photoluminescence spectroscopy. Usually increasing the size of QDs, their UV absorption and PL get shifted to a longer wavelength. The size of In(Zn)P/ZnS core/shell (CS) NCs increased as the reaction time increases. In addition the amount of myristic acid influences the size of the QDs is well known and observed during the research. In order to concentrate the effect of QD size on the optical property, the amount of MyA was optimized to 3.28 mmol. As the reaction time increases it is obvious that their absorption and PL λ_{max} is red-shifted. As shown in Fig 12, 13, and 14, with increasing the reaction time from 40 sec, 50 sec and 20 min, their PL λ_{max} is red-shifted 516 nm, 518 nm and 600 nm, respectively. It is observed there is a time limit for the growth of QD size. After 20 min the color does not shift to the longer wavelength any more.

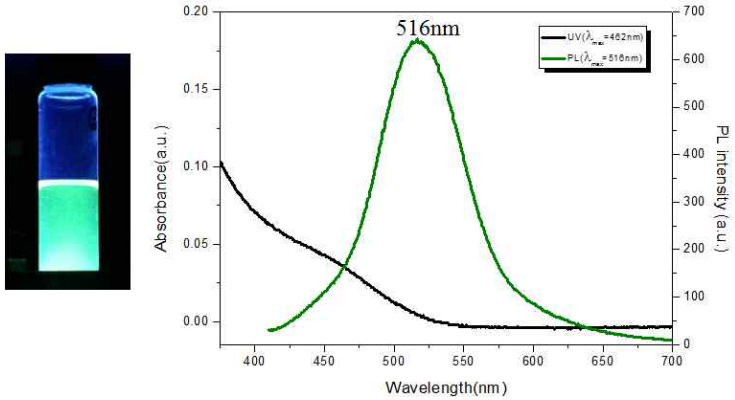

Fig. 12. Photo taken under the 365 nm UV radiation (Left), and UV-vis and PL spectra (Right) of In(Zn)P/ZnS core/shell (CS) NCs: reaction composition and condition of $In(OAc)_3$: $P(TMS)_3$ 1 : 1 (0.8 mmol : 0.8 mmol) , myristic acid 3.28 mmol , and reaction time 40 s.

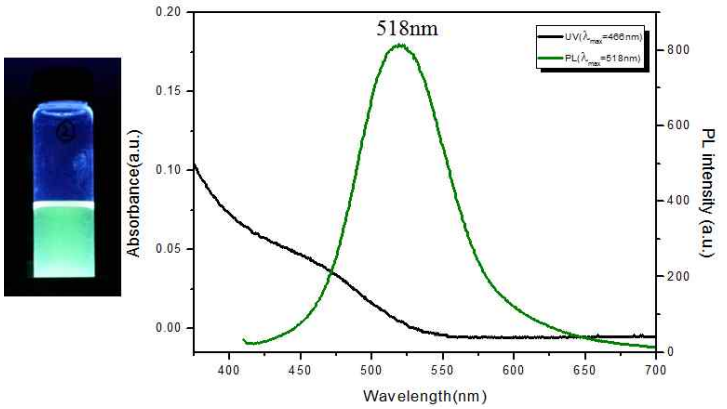

Fig. 13. Photo taken under the 365 nm UV radiation (Left), and UV-vis and PL spectra (Right) of In(Zn)P/ZnS core/shell (CS) NCs: reaction composition and condition of $In(OAc)_3$: $P(TMS)_3$ 1: 1 (0.8 mmol : 0.8 mmol), Myristic acid 3.28 mmol , Reaction time 50 s.

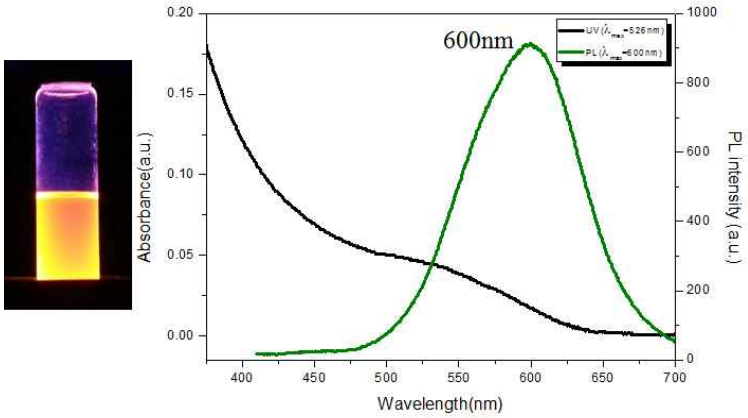

Fig. 14. Photo taken under the 365 nm UV radiation (left), and UV-vis and PL spectra (right) of In(Zn)P/ZnS core/shell (CS) NCs: reaction composition and condition of $In(OAc)_3$: $P(TMS)_3$ 1 : 1 (0.8 mmol : 0.8 mmol) , Myristic acid 3.28 mmol , Reaction time 20 min.

When In(Zn)P/ZnS core/shell (CS) NCs growth was stopped at 40 sec, it exhibited a pale green emission with λ_{em_max} 516 nm. The sample that was stopped at 50 sec exhibited a greener emission with with λ_{em_max} 518 nm is exhibited, and stopped at 20 min an orange with λ_{em_max} 600 nm, as shown in Fig. 12, 13, and 14, respectively. This demonstrates a successful control of shape to achieve differentiation in emission maxima within In(Zn)P/ZnS core/shell (CS).

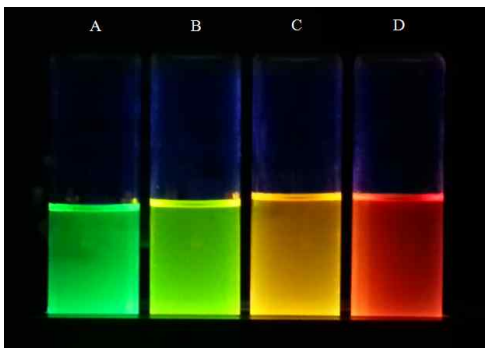

Fig. 15. Photos of different colors emitted by In(Zn)P/ZnS QDs under 365 nm UV irradiation. (**A**) λ_{em} = 516 nm (**B**) 532 nm (**C**) 564 nm (**D**) 600 nm

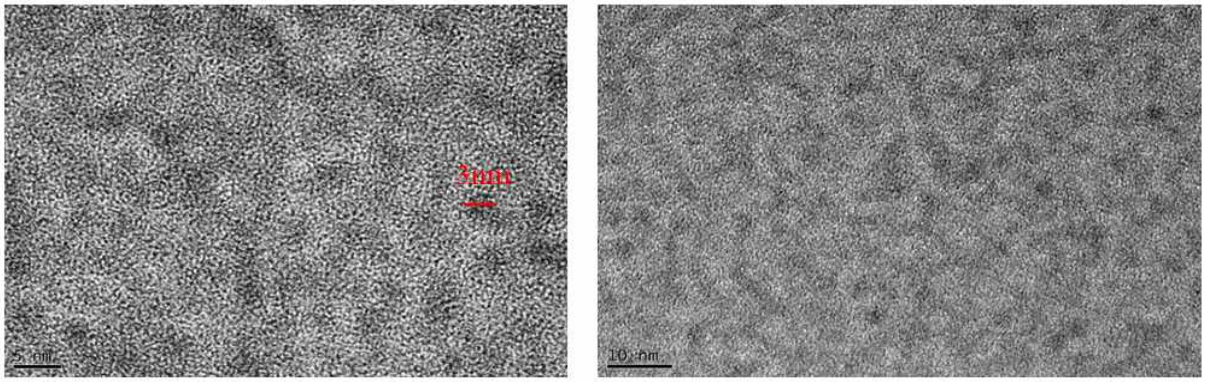

Fig. 16. TEM image of In(Zn)P/ZnS core/shell green emitting QDs with 4 shells, reaction time, 40 sec.

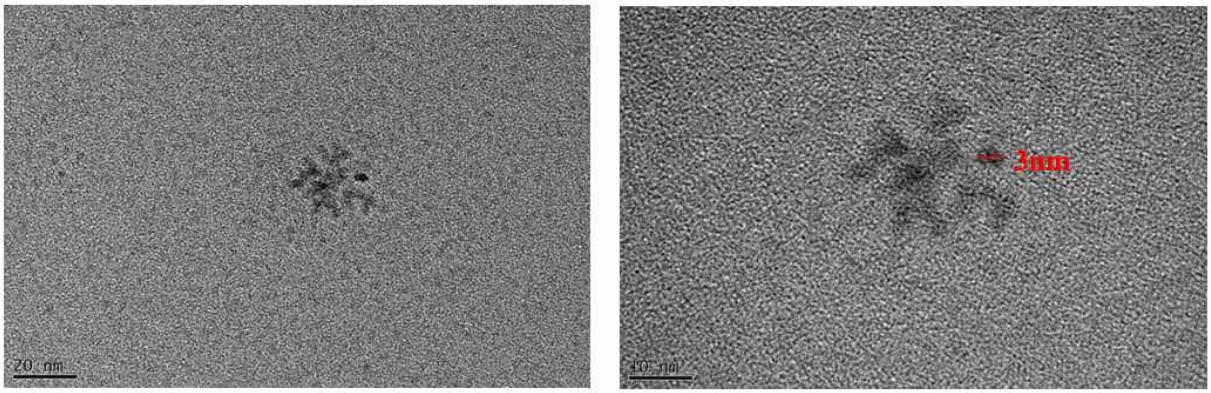

Fig. 17. TEM image of In(Zn)P/ZnS core/shell red yellow green QDs / 1 shells, reaction time, 50 sec.

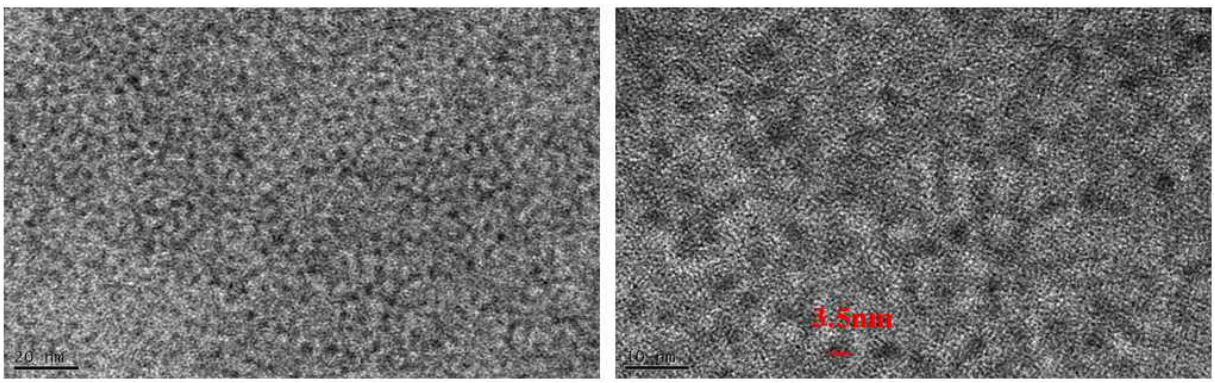

Fig. 18. TEM image of In(Zn)P/ZnS core/shell orange emitting QDs / 4 shells, reaction time, 30 min.

4-3. Influence of shell thickness

The control of the shell thickness is a delicate point in the fabrication of CS NCs and deserves special attention. If the shell is too thin, the passivation of the core NCs will be inefficient, resulting in reduced photostability. In the opposite case, the optical properties of the resulting CS NCs generally deteriorate as a consequence of strain induced by the lattice mismatch of the core and shell materials, accompanied by the generation of defect states. Using successive ion layer adsorption and reaction (SILAR) method on CdSe/CdS and CdS/ZnS QDs it was reported that PL QY of the core/shell nanocrystals increased as the shell thickness increased.[43] Such a detailed structural characterization and precise determination of the shell thickness are lacking in most III-V QD related reports. The latter is obviously complicated by the increased size distribution of the core InP NCs as compared to their II–VI semiconductor counterparts.[56]

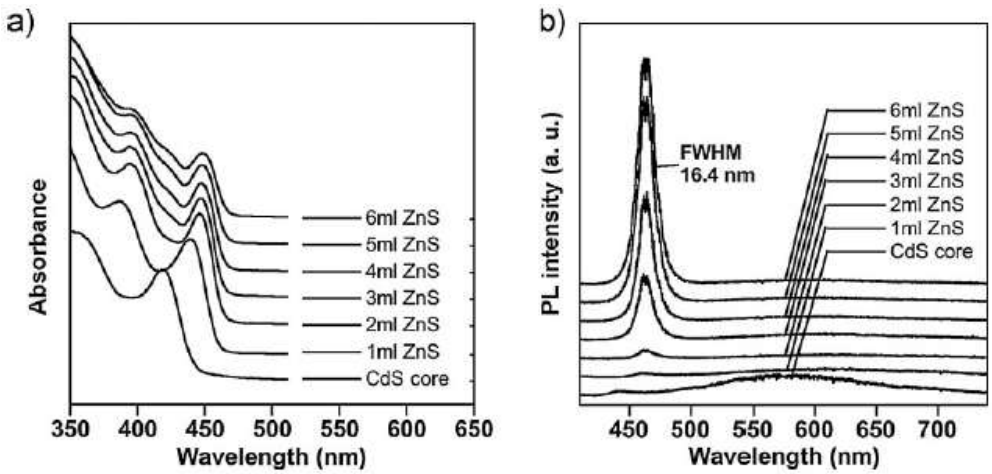

Fig. 19. a) UV/ Vis absorption spectra; b) PL spectra recorded during the addition of 6mL of the ZnS precursor solution corresponding to the growth of a 5-monolayer-thick ZnS shell on 4-nm CdS core NCs. Figure taken from reference 45

In this regard a study on increasing size distribution of ZnS shell over InP core was done by growing different size shells following SILAR method. Initially over a

green emitting InP core a 0.1 M solution of Zn and S precursors (both 1.2 mL each) were added at 150 ^{o}C to grow a single layer of shell. For the shell growth the reaction temperature was raised to 220 ^{o}C over a period of 30 minutes. Another sample with 0.2 M solution of Zn and S precursors (both 1.2 mL each, single layer) were made and analyzed for the absorption and emission. Samples with different shell thickness by two, three, four, and five successive addition of the 0.2 M solution of Zn and S precursors (both 1.2 mL each) were made and analyzed for the absorption and emission characteristics. Summary of the results are depicted in figure 19. As expected the shell growth is accompanied by a small red shift of the excitonic peak in the UV/Vis absorption spectrum and the photoluminescence (PL) wavelength. For the reaction with 0.1 M shell precursor solutions producing single layer shell where observed with unusually high PL QY compared to that of the 0.2 M shell precursor solutions producing single, double and triple shells. While the single shell with 0.1 M solutions of precursors is giving a quantum yield of 15 %, the highest obtained quintuple shell with 0.2 M solution showed a quantum yield of 20 %. Exact measurements of the shell thickness and its relation with QY are in progress along with other studies such as the effect of shells with 0.1 M precursor solutions producing multiple layers of shells and 0.2 M shell precursor solutions producing over six layers of shells.

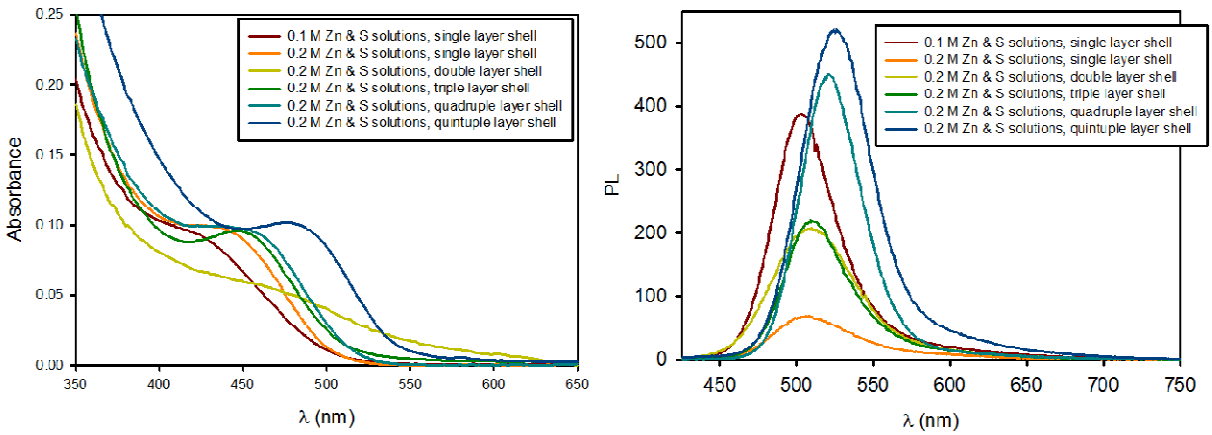

Fig. 20. UV-vis and PL spectra of samples with different ZnS shell thickness over InP emitting green color.

For In(Zn)P/ZnS core/shell (CS) NCs, the effect of shell thickness was investigated with ZnS shell component. In(Zn)P/ZnS core/shell (CS) NCs synthesized according to ***3-1-6.*** *Method-8* are measured varying the thickness of ZnS shell. Thickness of shell of In(Zn)P/ZnS core/shell (CS) NCs varied from1 to 8. Started from 1 to the 4 their QY increased 8 %, 14 %, 21 % and 30 %, as shown in Table 1. While, increasing the layers of ZnS shell from 5 to 8 decreases the emitting efficiency as shown in Fig. 21. It implies that the shell thickness enables increasing the optical efficiency.

Table 1. The reaction conditions for different shell thickness. Shell thickness from 1 to 4.

C/S	C/S/S	C/S/S/S	C/S/S/S/S
① $In(OAc)_3$ + MyA + ODE(10ml)	① $In(OAc)_3$ + MyA + ODE(10ml)	① $In(OAc)_3$ + MyA + ODE(10ml)	① $In(OAc)_3$ + MyA + ODE(10ml)
② PTMS + $Zn(Str)_2$	② PTMS + $Zn(Str)_2$	② PTMS + $Zn(Str)_2$	② PTMS + $Zn(Str)_2$
③ Sulfur + ODE(3ml) + $Zn(Str)_2$	③ Sulfur + ODE(3ml) + $Zn(Str)_2$	③ Sulfur + ODE(3ml) + $Zn(Str)_2$	③ Sulfur + ODE(3ml) + $Zn(Str)_2$
①+② 300°C (30min), cool down(10min)+③ 300°C (2h)	①+② 300°C (30min), cool down(10min)+③ 220°C (30m) + cool down(10min)+③ 220°C (30m)	①+② 300°C (30min), + cool down(10min)+③ 220°C (30m) + cool down(10min)+③ 220°C (30m)+cool down(10min)+③ 220°C (30m)	①+② 300°C (30min), cool down(10min)+③ 220°C (30m)+ cool down(10min)+③ 220°C (30m)+cool down(10min)+③ 220°C (30m)+cool down(10min) +③ 220°C (30m)
QY=8%	**QY=14%**	**QY=21%**	**QY=30%**
			

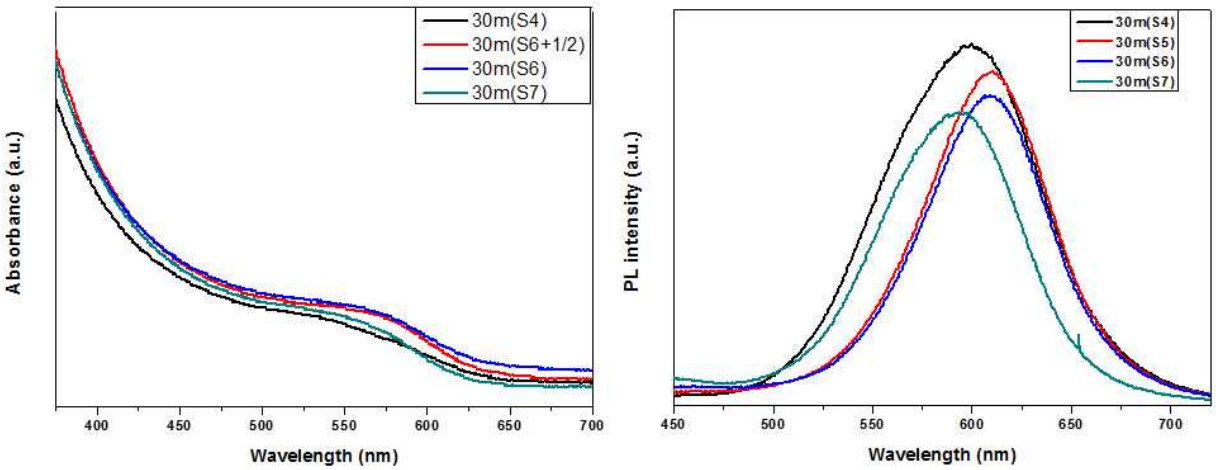

Fig. 21. UV-vis and PL spectra of red emitting In(Zn)P/ZnS core shell QDs with different shell layers from 5 to 8.

4-4. Influence of core/shell/shell (CSS) type InP/ZnSe/ZnS NC structures

The influence of shell thickness on QY originates from the lattice-mismatch of core material with the shell. The lattice mismatch value between InP and ZnS is high (~7 %). So the difficulty to respond simultaneously to the requirements of appropriate electronic (bandgap, band alignment) and structural (lattice mismatch) parameters for most binary CS systems was the motivation to synthesize NCs containing multiple shells. In particular the lattice mismatch between the core and the shell material strongly limits the possibility to grow a shell with significant thickness without deteriorating the photoluminescence properties. The use of a strain-reducing intermediate shell sandwiched between the core NC and an outer shell has first been proposed in the core/shell/shell (CSS) systems such as CdSe/ZnSe/ZnS.[57,58] The energy band of the intermediate shell is in such a way that it is higher than that of the core but lower than that of the outer shell so that the type-I structure is preserved without alteration. The interest of such structures lies in the combination of low strain, provided by the intermediate layer serving as a ‘‘lattice adapter’’ and efficient passivation and charge-carrier confinement assured by the outer shell. In the case of CdSe/ZnSe and CdSe/ZnS the CSS system offers higher stability against photo-oxidation than the CS

system and higher QYs than in the CS system of as evidenced by Talapin and co-workers who also extended this approach to CdSe/CdS/ ZnS CSS NCs.[59] For an InP system its lattice mismatch with ZnSe is only ~3.5 % and that between ZnSe and ZnS is 5 %. The bulk bandgap value for ZnSe (2.70 eV) is lower than that of ZnS (3.88 eV) and higher than that of InP (1.344 eV), which also makes it comfortable to choose ZnSe as the lattice adapter.

A InP/ZnSe/ZnS CSS system was attempted. In order to prepare the ZnSe shell, a 0.1 M zinc stearate solution in ODE and 0.1 M Se solution in TOP was used (1.2 mL each) at 150 ^{o}C. After allowing the shell growth at 220 ^{o}C for 30 minutes, the reaction mixture was brought down to 150 ^{o}C again for the addition of Zn and S precursor solutions. For the ZnS layer growth the reaction was brought to 220 ^{o}C for 30 minutes. Various combinations of Zn and Se precursor and various layers of ZnSe and ZnS by SILAR method were attempted. None of them produced any increase in QY, instead a quenching of QY was observed. The samples are presently being analyzed thoroughly for understanding the combinations and structure for further studies.

As this method has failed to give an admirable result, an alternative Se utilization was designed using elemental Se dispersed in 1-octadecene. A selenium stock dispersion was prepared by heating a calculated amount of elemental selenium in 1-octadecene at elevated temperatures for several hours. Experiments utilizing this stock solution are under progress.

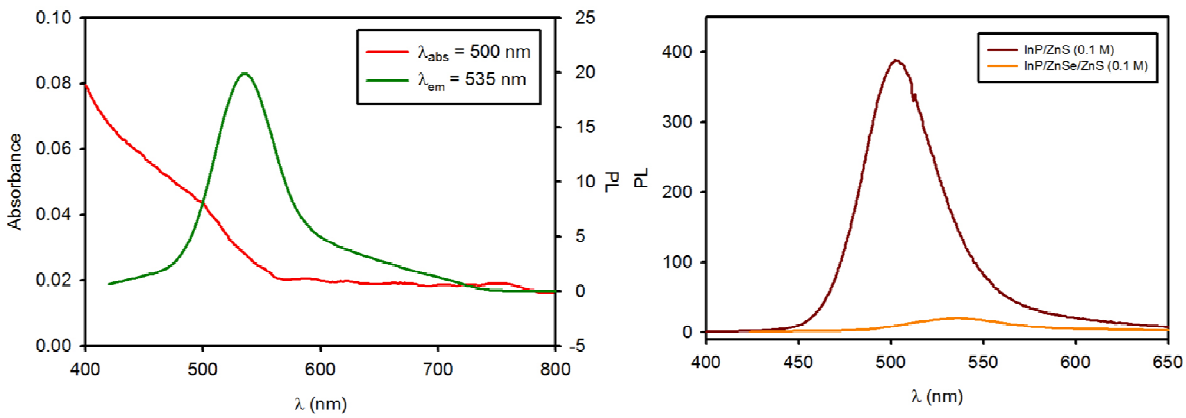

Fig. 22. UV-vis and PL spectra of InP/ZnSe/ZnS and comparison of PL spectra of InP/ZnS and InP/ZnSe/ZnS.

4-5. Surface passivation of InP/ZnS core/shell NCs with simple inorganic metal-free ligands

Despite progress in NC synthesis, fabrication of competitive solid-state devices from solution-processed colloidal building blocks remains challenging. In a NC solid, where each individual NC carries size dependent properties of the respective metal, semiconductor, or magnet, the transport of charges is dominated by the interparticle medium. The most successful synthetic methodologies developed for colloidal nanomaterials use surface ligands to stabilize the particles with long (C8 to C18) hydrocarbon chains or bulky organometallic molecules. These large molecules create highly insulating barriers around each NC. Complete removal of surface ligands has proven to be difficult and can create surface dangling bonds and charge-trapping centers. It would be beneficial to design surface ligands for colloidal nanostructures that adhere to the NC surface and provide colloidal stabilization, which can also provide stable and facile electronic communication between the NCs. Moreover this can constructively supplement the properties of the NC solid. We propose a generalized approach that is compatible with existing methodology for NC synthesis and is based on exchange of the original organic ligands with molecular metal free chalcogenide complexes. They provide colloidal stabilization of various nanostructures while enabling strong electronic coupling in the NC solids.

For this study S^{2-} and HS^{-} ligands were selected since reactions with these ligands could be done even at normal atmosphere. For the reaction QDs were taken as toluene solutions (~2 mg/mL) was mixed with a formamide solution of K_2S (~5 mg/mL) in a 10 mL glass vial. This was sonicated for a period of 10~15 minute, until the color of the toluene layer was completely transferred to the formamide layer.

The UV-vis and PL spectra of the formamide layer revealed that there is no considerable change in absorption or emission wavelength and their intensities. Further examination of these core/shell structures with inorganic metal free ligands are going on.

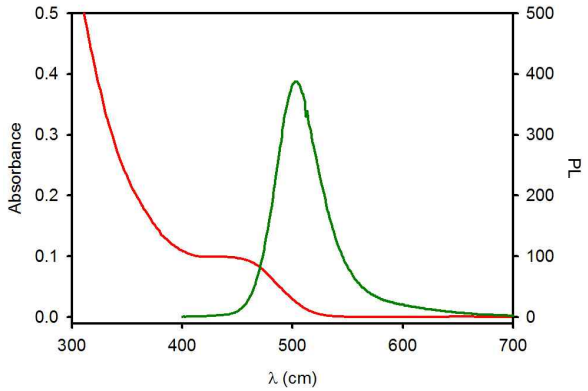

Fig. 23. UV-vis and PL spectra of green emitting InP/ZnS NCs with S^{2-} surface ligands in formamide.

4-6. Synthesis and characterization of InP/ZnS core/shell NCs doped with Ce^{3+} ions

Synthesis of doped semiconductor nanocrystal quantum dots (d-dots) have recently become an active subject in the field of materials chemistry because of their unique optical, electronic, and magnetic properties. The d-dots can not only retain nearly all advantages of intrinsic quantum dots but also eliminate their self-quenching due to reabsorption/energy transfer, greatly enhance their thermal stability, and significantly improve their chemical stability. In addition, d-dots might also offer high performance emissive materials without any highly toxic Class A elements (Cd, Hg, and Pb) to replace the current workhorse of intrinsic quantum dot emitters, CdSe-based NCs. Despite the recent advancement on synthetic chemistry of colloidal d-dots, successful doping that yielded highly emissive d-dots has been limited to the systems with II-VI semiconductor nanocrystals as the hosts. However, if excluding Cd and Hg as one of the elements, only zinc chalcogenide nanocrystals (typically ZnSe, ZnS, and ZnO) are the possible choices as II-VI semiconductor nanocrystal hosts, which shall have a very limited absorption and emission wavelength range for developing high performance d-dots emitters because of their relatively wide bandgap. On the contrary, III-V semiconductor nanocrystals can offer several narrow bandgap hosts without any Class A elements. It has been well-known that synthetic chemistry of intrinsic III-V

semiconductor nanocrystals is substantially different from and more difficult than that for II-VI ones. As for III-V d-dots, the knowledge has been quite limited. Several papers reported growth of Mn-doped III-V semiconductor nanocrystals for spintronics purposes, and the resulting d-dots only showed bandgap emission. Triply ionized rare earth (RE) elements also have magnetic properties due to their partially filled 4*f* shells, which are well screened by outer closed $5s^2$ and $5p^6$ orbitals. For this reason, the intracenter transitions of 4*f* electrons give rise to sharp emission spectra in various host materials. Luminescent lanthanide doped nanocrystals are unique in that they can convert low-energy radiation (typically near infrared) to higher energies such as visible or UV via a process known as upconversion.[44] Up conversion ability of NCs helps them to act like IR antenas in hybrid PV devices. RE ions doped IlI-V compound semiconductors were reported before either by diffusion of RE ions to III-V semiconductor thin films or by molecular beam epitaxy (MBE), to find potential applications in silica fiber based optical communication systems. According to the colloidal synthesis of transition metal:InP d-dots is reported before, apart from the bandgap emission a new dopant PL is originated at a lower energy region. Depending on the amount of dopant the bandgap emission of InP disappear and the dopant PL become the dominant. A similar observation is expected for the RE:InP d-dots.

There is no colloidal synthesis of RE doped III-V NCs reported so far and hence an attempt towards this direction was made to prepare RE: InP d-dots as industrially useful efficient color tunable emitters. The synthetic protocol is as depicted in figure 23.

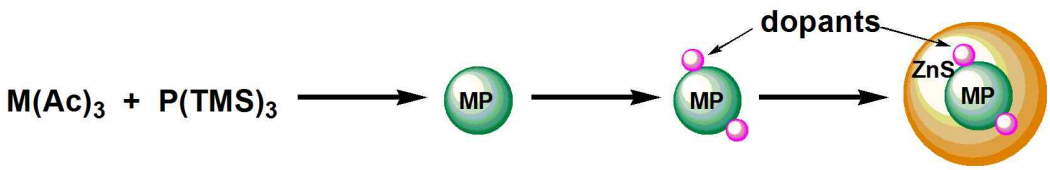

Fig. 24. Three step syntheses for doping colloidal semiconductor nanocrystals in one-pot protocol. InP spherical nanocrystal cores are made in colloidal method, rare-earth impurities are doped over them and it is followed by the growth of a ZnS shell.

For the preliminary attempts to produce doped III-V system Ce^{3+} ions were selected due to their easy availability. Cerium acetate is insoluble in 1-octadecene. A turbid dispersion of cerium acetate was prepared (5 %, 7 %, 10 % and 12 % with respect to indium) in 1-octadecene by heating a mixture to 250 ^{o}C under vigorous stirring and the heating and vigorous stirring was continued until the time of addition. InP core was prepared according the Method-2 described before. After the desired core growth time the reaction mixture was cooled to 150 ^{o}C and the turbid cerium acetate dispersion was added to the reaction mixture. The core growth was restricted to green emitting NCs since a further low energy PL was expected for that originating from dopant ions. After the addition the reaction mixture was heated to 220 ^{o}C for 30 minutes for the diffusion of Ce^{3+} into the InP crystal lattice. After the reaction time the reaction mixture again cooled to 150 ^{o}C for the shell growth. Precursors for shell growth were added and the temperature was again raised to 220 ^{o}C for shell growth. Multiple shell growth were attempted for preventing the doped RE ions escape from the core by diffusion.

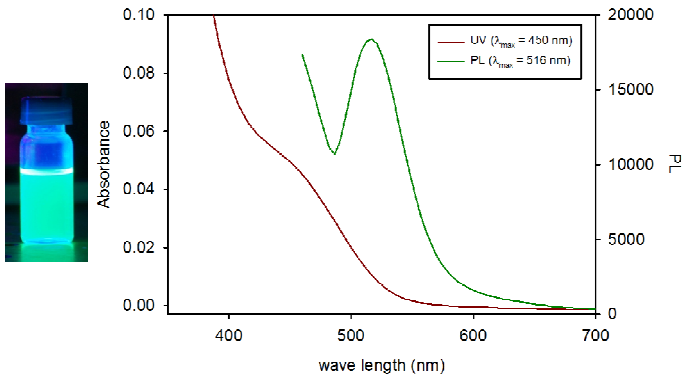

Fig. 25. UV-vis and PL spectra of Ce^{3+}(5 %):InP/ZnS green emitting d-dots synthesis reaction.

Detailed analysis of the doped structures revealed the presence of large lumps of possibly undissolved and unreacted cerium acetate in the samples indicating the inefficiency of this method to produce d-dots.

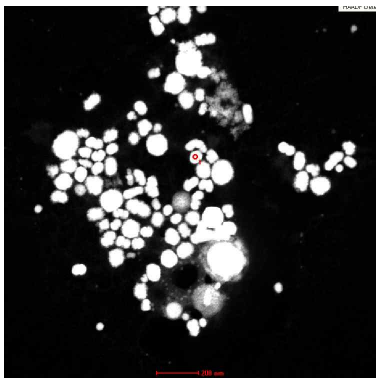

Fig. 26. UV-vis and PL spectra of Ce^{3+}(5 %):InP/ZnS green emitting d-dots synthesis reaction.

It was reported before that the reaction temperature has influence on the diffusion of dopants in the NC cores.[46] Xie and coworkers has showed that with temperature to be a key factor in successful doping of InP nanocrystals. They have found that with the increase of temperature lattice diffusion of dopants increases into the core. Based on this result, we have decided to go for a high temperature reaction to induce doping of RE elements into the InP core. To have a 300 ^{o}C reaction temperature, it is necessary to increase the amine alkyl chain length. Hexadecyl amine was chosen due to its high boiling point (330 ^{o}C) and low melting point (43 ^{o}C). When using the hexadecyl amine, the reaction mixture was found difficult to disperse in solvents after the reaction.

4-7. Synthesis and Characterization of InP/ZnS NCs doped with IIB, VIIB and Er

Based upon the above observation for Ce ion, Er and Mn is doped to the In(Zn)P core according following the same process described before. Er ion has been known a good light harvesting element and Mn is chosen its nontoxicity and availibity. A turbid dispersion of Erbium acetate was prepared (5 %, 7 % and 10 % with respect to indium) in 1-octadecene by heating a mixture to 250 ^{o}C under vigorous stirring and the heating and vigorous stirring was continued until the time of addition. In(Zn)P core was prepared according the Method-7 described before. After the desired core growth time the reaction mixture was cooled to 150 ^{o}C and the turbid cerium acetate dispersion was

added to the reaction mixture. The core growth was restricted to green emitting NCs since a further low energy PL was expected for that originating from dopant ions. After the addition the reaction mixture was heated to 220 ^{o}C for 30 minutes for the diffusion of Er^{3+} into the In(Zn)P crystal lattice. After the reaction time the reaction mixture again cooled to 150 ^{o}C for the shell growth. Precursors for shell growth were added and the temperature was again raised to 220 ^{o}C for shell growth. Multiple shell growth were attempted for preventing the doped RE ions escape from the core by diffusion.

Er-doped In(Zn)P/ZnS NCs emitted the green light, λ_{max} = 532 nm under the 365 UV irradiation with high optical efficiency as shown in Fig. 27. Also Er-doped QDs are to have smaller bandgap than the undoped In(Zn)P/ZnS QDs. Er-doped QDs has the size around 2.5 nm TEM (Fig. 28). The QDs spreads well evenly due to the introduction of even a single shell.

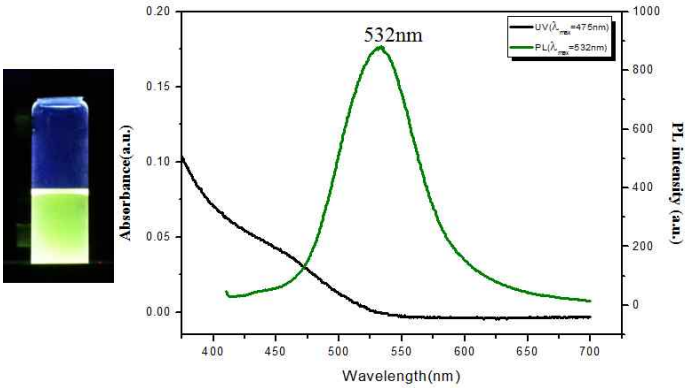

Fig. 27. UV-vis and PL spectra of Mn^{3+}(10 %):In(Zn)P/ZnS green emitting d-dots synthesis reaction.

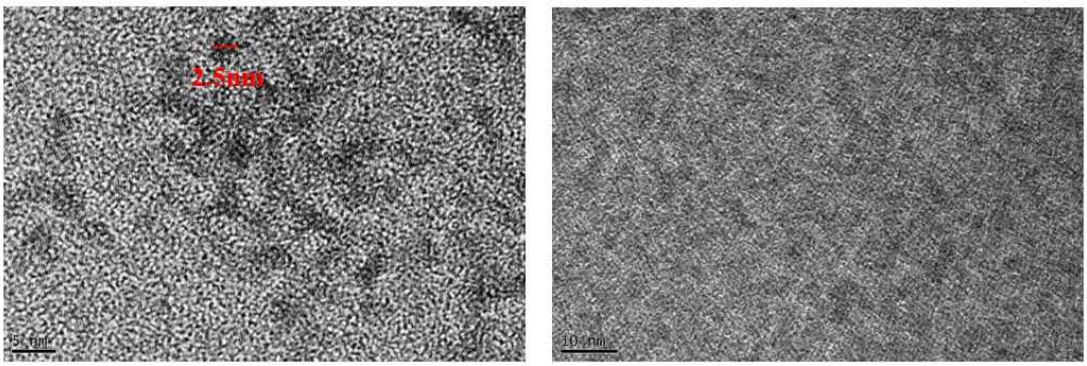

Fig. 28. TEM image of Mn^{3+}(10 %):In(Zn)P/ZnS green emitting QDs / 1 shell, reaction time 40 sec, Manganese(III) acetate (10%)

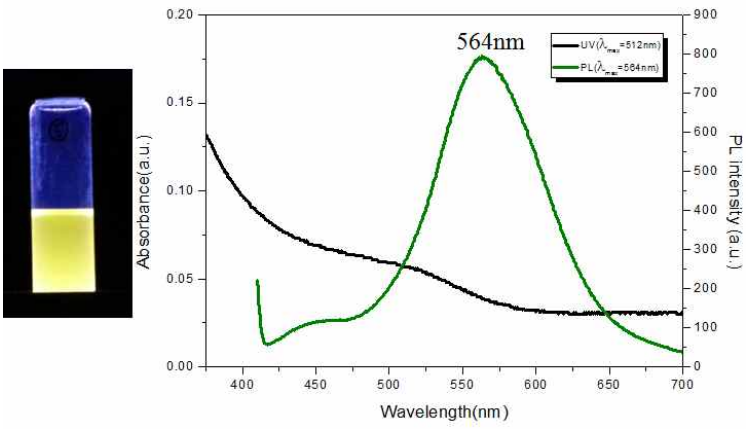

Fig. 29. UV-vis and PL spectra of Er^{3+}(10 %):In(Zn)P/ZnS yellow green emitting d-dots synthesis reaction.

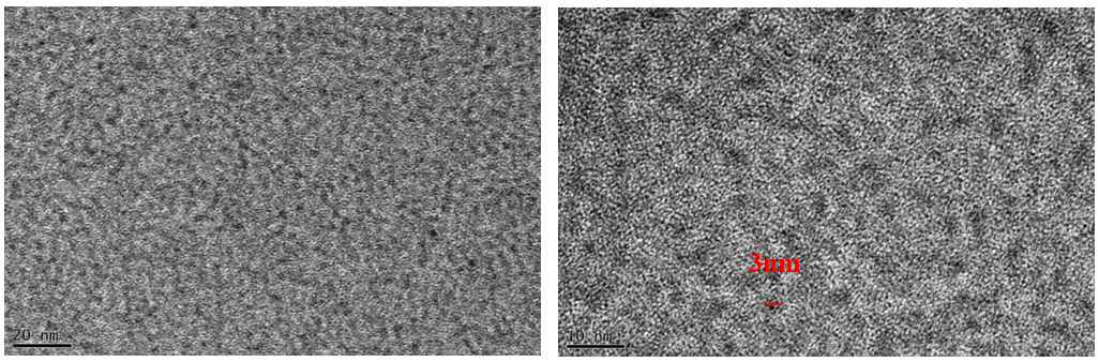

Fig. 30. TEM image of Er^{3+}(10 %):In(Zn)P/ZnS yellow green emitting d-dots QDs /1 shell, reaction time 40 sec, Erbium(III) acetate (10%).

When In(Zn)P/ZnS core/shell QDs are doped, their PL intensity substantially increased as shown in Fig. 31. In comparison with Er^{3+} and Mn^{3+} doped In(Zn)P/ZnS core/shell QDs, Erbium d-dot shows more enhanced intensity in PL spectra. Doping has influence on both the optical properties and the size of d-dots.

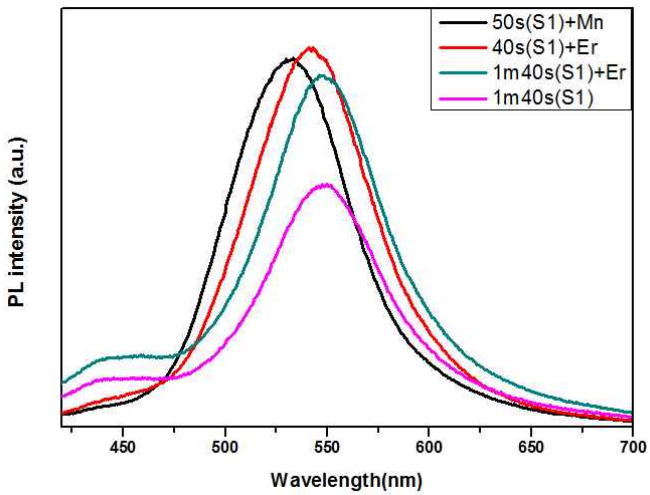

Fig. 31. PL spectra of In(Zn)P/ZnS core shell red QDs with different doping elements, Er and Mn.

6. Summary and outlook

Aim of this work is to prepare rare earth (RE) metal doped Cd free quantum dots (eg, RE:InP/ZnS) with nontoxicity and efficient light emitting activity, and further enhancement of their PL by reducing quenching due to the surface defects by a combination of efficient core/shell (CS) and core/shell/shell (CSS) structures. These CS or CSS d-dots are planned to surface passivation with inorganic metal-free ligands for efficient electron-hole injection for a better utilization in display devices. Each of the ideas were attempted to standardize separately. Among them InP/ZnS core/shell structures were successful prepared from a low temperature amine ligand based process. Emission color tuning was also successfully done with these NCs over all color range. Synthetic protocol for other group III element phosphides is in process of design. Doping with Ce^{3+} was attempted over InP/ZnS CS structure. Attempt at 180 ^{o}C was not successful and hence attempts to develop high temperature reactions are in progress. InP/ZnS CS systems with multiple shells up to five shell layers were prepared and the increasing number of layers was found to influence the PL quantum yield positively. Further experiments are in process to optimize the shell thickness. InP/ZnSe/ZnS CSS system under various conditions of Se solutions was attempted. Ligands used for Se

solvation in ODE were found to affect the nanocrystal growth and hence a method to prepare elemental Se clear dispersion was adapted from literature and reactions with the clear dispersion are in progress. Surface passivation of InP/ZnS with inorganic metal free ligands was done successfully.

Systematic attempt to synthesize the QDs having various components in their core lattice and to endow better stability by changing shelling materials and layers has widely performed. Novel In(Zn)P/ZnS core-shell QDs as well as In(Zn)P/ZnS d-dots containing Ce, Er, and Mn have successfully realized and characterized. Among the doping materials Erbium exhibited the highest PL intensity. Their color tunings are able to be realized by fine reaction time control from 40 sec to 20 min and green to orange colors, respectively. For shell thickness d-dots with 1 to 8 shells were investigated. Increasing shell thickness the quantum yield increases from 1 to 4 shells and then begins to decrease from 5 up to 8 layers. PL intensity showed maximum quantum yield at 4 shells.

B6. Reference

(1) Bruchez Jr, M.; Moronne, M.; Gin, P.; Weiss, S.; Alivisatos, A. *Science* **1998**, *281*, 2013.

(2) Chan, W.; Nie, S. *Science* **1998**, *281*, 2016.

(3) Kim, S.; Lim, Y. T.; Soltesz, E. G.; De Grand, A. M.; Lee, J.; Nakayama, A.; Parker, J. A.; Mihaljevic, T.; Laurence, R. G.; Dor, D. M.; Cohn, L. H.; Bawendi, M. G.; Frangioni, J. V. *Nat Biotech* **2004**, *22*, 93.

(4) Michalet, X.; Pinaud, F.; Bentolila, L.; Tsay, J.; Doose, S.; Li, J.; Sundaresan, G.; Wu, A.; Gambhir, S.; Weiss, S. *Science* **2005**, *307*, 538.

(5) Colvin, V.; Schlamp, M.; Alivisatos, A. *Nature* **1994**, *370*, 354.

(6) Klimov, V.; Mikhailovsky, A.; Xu, S.; Malko, A.; Hollingsworth, J.; Leatherdale, C.; Eisler, H.; Bawendi, M. *Science* **2000**, *290*, 314.

(7) Guyot-Sionnest, P. *C. R. Phys.* **2008**, *9*, 777.

(8) Xie, R.; Battaglia, D.; Peng, X. *J. Am. Chem. Soc* **2007**, *129*, 15432.

(9) Matsuoka, T.; Okamoto, H.; Nakao, M.; Harima, H.; Kurimoto, E. *Appl. Phys. Lett.* **2002**, *81*, 1246.
(10) Strite, S.; Morkoc, H. *J. Vac. Sci. Technol. B* **1992**, *10*, 1237.
(11) Monemar, B. *J. Mater Sci.* **1999**, *10*, 227.
(12) Chitambar, C. *Curr. Opin. Oncol.* **2004**, *16*, 547.
(13) Even-Sapir, E.; Israel, O. *Eur. J. Nucl. Med. Mol. I.* **2003**, *30*, 65.
(14) Seregni, E.; Chiti, A.; Bombardieri, E. *Eur. J. Nucl. Med. Mol. I.* **1998**, *25*, 639.
(15) Cao, Y.; Banin, U. *J. Am. Chem. Soc* **2000**, *122*, 9692.
(16) Micic, O.; Cheong, H.; Fu, H.; Zunger, A.; Sprague, J.; Mascarenhas, A.; Nozik, A. *J. Phys. Chem. B* **1997**, *101*, 4904.
(17) Qiu, H.; Cao, C.; Zhu, H. *Mater. Sci. Eng: B-Adv.* **2007**, *136*, 33.
(18) Liu, W.; Zhou, H.; Fang, C.; Wang, M.; Zhang, Y.; Chen, Z.; Che, P. *Rare Metals* **2010**, *29*, 138.
(19) Chan, W.; Maxwell, D.; Gao, X.; Bailey, R.; Han, M.; Nie, S. *Curr. Opin. Biotech.* **2002**, *13*, 40.
(20) Ng, K. *Complete guide to semiconductor devices*; Wiley Online Library, 1995.
(21) Dai, Q.; Song, Y.; Li, D.; Chen, H.; Kan, S.; Zou, B.; Wang, Y.; Deng, Y.; Hou, Y.; Yu, S. *Chem. Phys. Lett.* **2007**, *439*, 65.
(22) Streetman, B.; Banerjee, S. *Solid State Electronic Devices*; 5th Edition ed.; Prentice Hall, New Jersey, 1999.
(23) Singh, J. *Physics of Semiconductors and their Heterostructures*; McGraw-Hill New York, 1993.
(24) Tiwari, S. *Compound semiconductor device physics*; Academic Pr, 1992.
(25) Lin, K.; Catchpole, K.; Campbell, P.; Green, M. *Semicond. Sci. Technol.* **2004**, *19*, 1268.
(26) Denzler, D.; Olschewski, M.; Sattler, K. *J. Appl. Phys.* **1998**, *84*, 2841.
(27) Wang, Z. *J. Phys-Condens. Mat.* **2004**, *16*, R829.
(28) Malik, M. A.; Afzaal, M.; O'Brien, P. *Chem. Rev.* **2010**, *110*, 4417.
(29) Ichimura, M.; Sato, N.; Nakamura, A.; Takeuchi, K.; Arai, E. *Phys. Status Solidi A* **2002**, *193*, 132.
(30) Xiao, J.; Xie, Y.; Tang, R.; Luo, W. *Inorg. Chem.* **2003**, *42*, 107.

(31) Kuykendall, T.; Ulrich, P.; Aloni, S.; Yang, P. *Nat. Mater.* **2007**, *6*, 951.

(32) Coe Sullivan, S.; Steckel, J.; Woo, W.; Bawendi, M.; Bulovi , V. *Adv. Funct. Mater.* **2005**, *15*, 1117.

(33) Mirkin, C. A.; Letsinger, R. L.; Mucic, R. C.; Storhoff, J. J. *Nature* **1996**, *382*, 607.

(34) Park, J.; Prabhakaran, P.; Jang, K.; Lee, Y.; Lee, J.; Lee, K.; Hur, J.; Kim, J.; Cho, N.; Son, Y. *Nano lett.* **2010**, 3822.

(35) Park, J.; Lee, K.; Joo, W.; Bulliard, X.; Choi, Y.; US Patent App. 20,100/117,110, 2009.

(36) Park, J.; Bulliard, X.; Lee, J.; Hur, J.; Im, K.; Kim, J.; Prabhakaran, P.; Cho, N.; Lee, K.; Min, S. *Adv. Funct. Mater.* **2010**, *20*, 2296.

(37) Hirata, S.; Lee, K.; Watanabe, T. *Adv. Funct. Mater.* **2008**, *18*, 2869.

(38) Cho, N.; Roy Choudhury, K.; Thapa, R.; Sahoo, Y.; Ohulchanskyy, T.; Cartwright, A.; Lee, K.; Prasad, P. *Adv. Mater.* **2007**, *19*, 232.

(39) Kim, W.; Kim, S.; Lee, K.; Samoc, M.; Cartwright, A.; Prasad, P. *Nano lett.* **2008**, *8*, 3262.

(40) Choudhury, K.; Kim, W.; Sahoo, Y.; Lee, K.; Prasad, P. *Appl. Phys. Lett.* **2006**, *89*, 051109.

(41) Choudhury, K.; Kim, W.; Sahoo, Y.; Lee, K.; Prasad, P.; Cartwright, A.; Thapa, R.; US Patent App. 20, 021, Ed., 2008.

(42) Hsieh, J., Tesis, Massachusetts Institute of Technology, 2010.

(43) Li,. J. J.; Wang, A.; Guo, W.; Keay, J. C.; Mishima, T. D.; Johnson, M. B.; Peng, X. *J. Am. Chem. Soc.* **2003,** *125,* 12567.

(44) Scheps, R. *Progress in Quantum Electron.* **1996**, *20*, 271.

(45) Reiss, P.; Protiére, M.; Li, L. *small* **2009**, *5*, 154.

(46) Xie, R.; Peng, X. *J. Am. Chem. Soc.* **2009**, *131*, 10645

List of Publications

1) K. K. Jang, P. Prabhakaran, D. Chandran, J.-J. Park, K.-S. Lee*, *Optical Materials Express*, **2(5)**, 519-525 (2012)
"Solution processible and photopatternable blue. Green and red quantum dots suitable for full color displays devices"
→Top Download Paper, Optical Society of America (OSA)

2) P. Prabhakaran, W. J. Kim, K.-S. Lee*, P.N. Prasad*, *Optical Materials Express*, **2(5)**, 578-593 (2012)
"Quantum dots for photonic applications"
→Top Download Paper, Optical Society of America (OSA)

3) S. H. Lee, H. Lee, S. Park, K. Kim, Y.-B. Lee, J. Kim, K.-S. Lee*, J. Joo*, *Synthetic Metals*, **163**, 1-6(2013)
"Hybrid effects of CdSe/ZnS quantum dots on p-n heterojunction organic nanowire"
→ Cover page paper

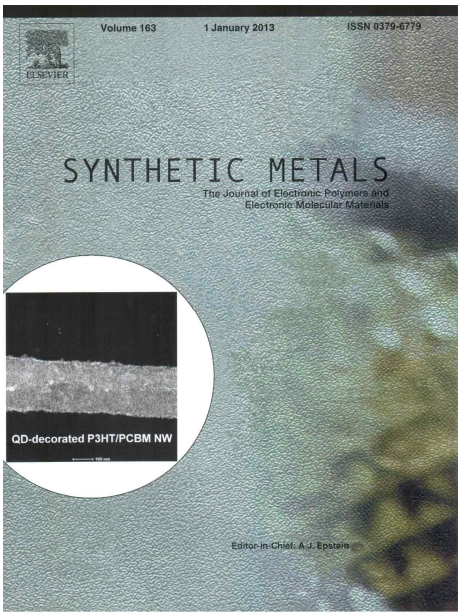

4) E. H. Cho, B.-G. Kim, S. Jun, J. Lee, D. H. Park, K.-S. Lee, J. Kim, J. Kim, J. Joo, *Advanced Materials*, submitted 2013.
"Polychromatic optical waveguide using blue-light-emitting organic nanowire hybridized with quantum dots"

5) D. Chandran, S. Jeon, K.-S. Lee, in preparation
"Stable and efficient group III-V semiconducting nanocrystals for optoelectronic applications"

List of Presentations

1) P. Prabhakaran, K. K Jang, S.-Y. Park, S.-M Jeon, K.-S. Lee, J.-J Park, Y. Son, D.-Y. Yang. "Metal and quantum dot containing patterns by two-photon lithography" 2012 Photonics West, San Francisco, California, USA, January 21~26, 2012. (Invited Lecture)

2) K.-S. Lee, "Quantum Dots for Photonic Applications", Korea-France Joint Symposium 2012, Ewha Womans University, Seoul, Korea, February 6~10, 2012. (Invited Lecture)

3) S.-M. Jeon, S.-Y. Park, J.-S. Joo, Y.-B. Lee, K.-S. Lee, "Synthesis and Application of Organic-Quantum Dot Hybrid Materials", 2012 Spring Meeting of the Polymer Society of Korea, Daejeon Convention Center, Daejeon, Korea, April 12~13, 2012.

4) K.-S. Lee, "3D Patterns Containing Quantum Dots and Metallic Nanoparticles for Photonic Applications", International Workshop on Novel Nanomagnetic & Multifunctional Materials 2012 (IW-NMM2012), Sheraton Walkerhill Hotel, Seoul, Korea, June 11~14, 2012. (Invited Lecture)

5) S.-M. Jeon, K.-S. Lee, S.-Y. Park, D. Chandran, "Alloy core/shell semiconducting nanocrystals of group III–V elements and their doped structures as highly luminescent nanomaterials", 2012 Annual Fall Meeting of the Polymer Society of Korea, Changwon Convention Center, Changwon, Korea, October 11~12, 2012.

6) K.-S. Lee, "3D Nano/Micro Patterns Containing Quantum Dots and Metallic Nanoparticles for Photonic Applications", International Conference on Emerging Advanced Nanomaterials 2012, Hotel Mercure Brisbane, Brisbane, Australia, October 22~25, 2012. (Keynote Lecture)

7) J. Joo, Y.-B. Lee, S.-H. Lee, Y.-D. Han, S.-M. Lee, S.-Y. Park, K.-S. Lee, J. Kim, "Quantum Dots and Organic Hybrid Nanostructures: Nanoscale Optical and Electrical Characteristics", International Conference on Science and Technology of Synthetic Metals 2012 (ICSM 2012), Atlanta, USA, July 8~12, 2012.

8) E.-H. Cho, H.-S. Lee, Y.-D. Han, B.-K. Kim, S.-Y. Park, J. Kim, K.-S. Lee, J. Kim, J. Joo, "Multi-Modes Waveguiding Property in Organic Nanowire-Quantum Dots Hybrid System and Charge Transfer between D-A Heterojunction using a Coaxial Nanowire", International Conference on Science and Technology of Synthetic Metals 2012 (ICSM2012), Atlanta, USA, July 8-12, 2012

9) K.-S. Lee, "2D and 3D Patterned Organic-Inorganic Hybrid Systems for Photonic Applications", German-Korean Polymer Symposium, Hamburg University, Hamburg, Germany, August 26~29, 2013. (Invited Lecture)